U.PORTO

FACULDADE DE CIÊNCIAS
UNIVERSIDADE DO PORTO

MSc

2.º CICLO

FCUP
ICBAS
IBMC
2014

U.PORTO

Dual regulation of Mps1 by Polo defines SAC robustness and responsiveness

Ana Catarina Barbosa

FC

U.PORTO

FACULDADE DE CIÊNCIAS
UNIVERSIDADE DO PORTO

U.PORTO

INSTITUTO DE CIÊNCIAS BIOMÉDICAS ABEL SALAZAR
UNIVERSIDADE DO PORTO

IBMC INEB
Laboratório Associado . Associate Laboratory

Dual regulation of Mps1 by Polo defines SAC robustness and responsiveness

Ana Catarina Correia Barbosa

Dissertação de Mestrado apresentada à
Faculdade de Ciências da Universidade do Porto,
Instituto de Ciências Biomédicas Abel Salazar
Bioquímica

2014

MSc

Dual regulation of Mps1 by Polo defines SAC robustness and responsiveness

Ana Catarina Correia Barbosa

Mestrado em Bioquímica

Departamento de Química e Bioquímica

2014

Orientador

Doutor Carlos Conde, IBMC

Coorientador

Professor Doutor Claudio Sunkel, IBMC

Todas as correções determinadas pelo júri, e só essas, foram efetuadas.

O Presidente do Júri,

Porto, _____/_____/_____

Agradecimentos

Ao terminar este projeto, gostaria de manifestar os meus sinceros agradecimentos a todos aqueles que, de alguma forma, contribuíram para que a realização deste objetivo fosse alcançada.

Quero começar por agradecer ao Professor Doutor Claudio Sunkel pela oportunidade de realizar este projeto no grupo de Genética Molecular do IBMC.

Um agradecimento especial ao Doutor Carlos Conde por me ter aceitado como orientanda, pelos conhecimentos científicos transmitidos ao longo destes meses e conselhos oportunos essenciais para o meu desenvolvimento profissional. Agradeço também pela motivação, disponibilidade, apoio e boa disposição, que foram sempre constantes ao longo deste período.

Quero também agradecer especialmente à Mariana Osswald por todo o apoio no laboratório, pelo conhecimento transmitido e por me fazer acreditar que tudo se consegue com motivação.

Agradeço também a todos os membros do laboratório de Genética Molecular pela hospitalidade, simpatia, ajuda e, acima de tudo, por me proporcionarem uma experiência muito gratificante a todos os níveis. Um sincero obrigada ao Miguel pelo companheirismo e por ter tornado esta experiência tão divertida.

Aos meus pais, um especial e sentido agradecimento, pelo apoio incondicional, compressão e amor que sempre demonstraram ao longo de toda a minha vida, mesmo com o meu mau feitio, fazendo-me crescer e acreditar que com esforço e dedicação tudo é possível.

Às minhas amigas e companheiras desta viagem Helena, Cristiana, Cleide, Rita e Inês por me darem força, limparem as lágrimas e terem sempre uma palavra amiga nos momentos menos bons e cansativos. E aos amigos e companheiros Celso, Martinho e João pelos almoços, lanches e jantares onde se discutia de tudo um pouco, inclusive ciência. Um muito obrigada!

Abstract

Maintenance of genomic stability during eukaryotic cells division relies on the spindle assembly checkpoint (SAC). The SAC is a surveillance mechanism that restrains anaphase onset until all chromosomes are correctly attached to microtubules from opposite spindle poles. Unattached kinetochores generate a 'wait-anaphase' signal by promoting the formation of the mitotic checkpoint complex (MCC), which efficiently inhibits the activity of the anaphase-promoting complex/cyclosome (APC/C) and prevents degradation of Cyclin B and Securin. A single unattached kinetochore is sufficient to halt mitotic progression. Remarkably, anaphase takes place swiftly after all kinetochores stably attach to spindle microtubules, revealing that the SAC is not only extremely robust, but also highly responsive. How the SAC encompasses simultaneously both features remains unclear.

Mps1 kinase is a key regulator of SAC signaling pathway due to its upstream role in MCC assembly. The accumulation of Mps1 at unattached kinetochores potentiates its auto-activation by trans-phosphorylation, which is necessary to achieve full kinase activity and sustained SAC function. Nevertheless the molecular mechanism by which Mps1 is recruited to kinetochores remains unclear. We found that depletion of Polo kinase in *Drosophila* S2 cells caused a substantial reduction of Mps1 recruitment to unattached kinetochores. However, if Polo activity was inhibited with BI2536 after mitotic entry, an increase of Mps1 levels at kinetochores was observed. Our results strongly suggest that this contradiction is explained by spatiotemporal specific requirements of Polo activity for Mps1 kinetochore localization. Polo activity is required during prophase to trigger Mps1 activation at the nuclear envelope/pore. This Polo-dependent activation of Mps1 is required to drive the initial recruitment of Mps1 to unattached kinetochores in early mitosis. Our biochemical data showed that Polo and Mps1 interact *in vivo* and that Polo is able to phosphorylate Mps1 N-terminal region *in vitro*, which led us to hypothesize that Polo could directly regulate Mps1 kinetochore recruitment and/or activity. To gain insight into the mechanisms by which Polo controls Mps1 we generated S2 cell lines expressing phosphomimetic and phosphodefective versions of Mps1 for Polo-dependent phosphorylation residues (Thr185, Thr197, Thr260 and Ser262).

In vivo analysis of mitotic progression through time-lapse confocal microscopy revealed that *Drosophila* S2 cells expressing EGFP-Mps1^{4A} (phosphodefective mutant) arrest in mitosis for longer periods of time (~ 8.6 hours) when compared to cells expressing EGFP-Mps1^{WT} (~ 6.6 hours), whereas cells overexpressing the phosphomimetic version EGFP-Mps1^{4D} spent on average ~ 3.7 hours in mitosis. These results suggest that Polo phosphorylation of Mps1 N-terminal region negatively regulates Mps1 activity and consequently SAC robustness. Analysis of Mps1 dynamics at unattached kinetochores by Fluorescence Recovery After Photobleaching (FRAP) showed that Polo inhibition caused a six-fold increase in the half-life of recovery of EGFP–Mps1^{WT}. This result indicates that Polo activity is required for Mps1 dynamic exchange at kinetochores and correlates with the increase in Mps1 kinetochore levels observed upon BI2536 addition. Interestingly, EGFP-Mps1^{4D} exhibited a two-fold decrease in the half-life of recovery relative to its wild-type counterpart hence indicating that the mechanism by which Polo controls Mps1 release from kinetochores likely involves phosphorylation of its N-terminal region by Polo.

The results presented in this thesis suggest that Polo exerts a dual control over Mps1 kinase. Polo promotes Mps1 activation at the nuclear envelope/pore and its subsequent nuclear import during prophase, which likely leads to auto-phosphorylation dependent Mps1 recruitment to prometaphase kinetochores required to establish a robust SAC response. Mps1 in its active conformation exposes its N-terminal domain that becomes phosphorylated by Polo. Polo-mediated phosphorylation of Mps1 N-terminal region restrains Mps1 activity and promotes its prompt dissociation from kinetochores. This allows fast SAC silencing upon biorientation, hereby providing SAC responsiveness.

Keywords: Polo, Mps1, SAC, Kinetochore, Mitosis, Regulation.

Resumo

O processo de divisão celular eucariota tem que ser rigorosamente regulado de modo a assegurar a estabilidade genómica da progenia. A fidelidade deste processo é assegurada pelo SAC, um mecanismo sensível à ligação de microtúbulos a cinetocoros, que impede a ativação do APC/C e a subsequente transição para anafase até que todos os cromossomas estejam corretamente ligados ao fuso mitótico. Um cinetocoro gera um sinal suficientemente forte na forma do MCC para inibir o APC/C e manter a célula em mitose. Por outro lado, a partir do momento em que todos os cinetocoros estão corretamente ligados ao fuso mitótico, o sinal inibitório deixa de ser produzido, o SAC é silenciado e a célula entra imediatamente em anafase. Isto significa que o SAC é simultaneamente robusto e sensível. Os mecanismos que fazem com que o SAC tenha simultaneamente estas duas características permanecem incompreendidos.

A cinase Mps1 é um importante regulador do SAC atuando a vários níveis da via de sinalização no sentido de promover a formação do MCC. Esta cinase acumula-se preferencialmente nos cinetocoros livres de microtúbulos. Esta localização potencia sua auto-ativação através da sua trans-fosforilação, o que é fundamental para a sua completa ativação e, assim, sustentar a função do SAC. Apesar do seu papel critico enquanto regulador do SAC, os mecanismos moleculares que controlam a localização e ativação de Mps1 nos cinetocoros permanecem pouco claros. Os resultados apresentados nesta tese mostram que a depleção da proteína cinase Polo em células S2 de *Drosophila* leva a uma redução significativa dos níveis de Mps1 no cinetocoro. No entanto, quando o Polo é inibido com BI2536 após entrada em mitose observa-se um aumento dos níveis de Mps1. Esta discrepância poder-se-á dever ao momento em que a perda de atividade Polo ocorre. Células depletadas de Polo entram em mitose na ausência de Polo. Por outro lado, em células tratadas com BI2536, a cinase Polo é inibida em células que já estão em mitose. Resultados apresentados nesta tese sugerem que o Polo ativa Mps1 ao nível do invólucro nuclear/poros nucleares e promove a incorporação de Mps1 ativo para o núcleo durante profase. Esta ativação inicial parece ser importante para permitir o recrutamento inicial de Mps1 para o cinetocoro. Experiências bioquímicas mostraram uma interação *in vivo* entre Polo e Mps1 e que Polo tem a capacidade de fosforilar o domínio N-terminal de Mps1 *in vitro*. Recorrendo a uma análise *in silico* identificamos quatro resíduos

putativamente fosforiláveis pelo Polo na região N-terminal de Mps1 (Thr185, Thr197, Thr260 e Ser262).

Para avaliar a relevância destas fosforilações geramos linhas celulares S2 a expressar versões mutadas de Mps1 que impedem (EGFP-Mps1^{4A}) ou mimetizam (EGFP-Mps1^{4D}) a fosforilação pelo Polo nos resíduos identificados na região N-terminal de Mps1. A análise da progressão mitótica *in vivo* revela que a linha celular que expressa EGFP-Mps1^{4A} permanece em mitose por um longo período tempo (~ 8,6 horas) comparativamente com células que expressam EGFP-Mps1^{WT} (~ 6.6 horas), enquanto as células que expressam EGFP-Mps1^{4D} apenas permanecem ~ 3.7 horas em mitose. Estes resultados indicam que a fosforilação no domínio N-terminal do Mps1 pelo Polo tem um impacto negativo na atividade da cinase. A análise da dinâmica de Mps1 por FRAP mostrou que a inibição de Polo causa um aumento dramático no tempo de retenção de Mps1 no cinetocoro. Este resultado sugere que a atividade do Polo é fundamental para o Mps1 seja removido do cinetocoro. No mesmo sentido, o EGFP-Mps1^{4D} apresenta um comportamento mais dinâmico nos cinetocoros que EGFP-Mps1^{WT} sugerindo que a fosforilação de Mps1 no N-terminal pelo Polo promove a remoção de Mps1 do cinetocoro.

Os resultados apresentados nesta tese permitem-nos propor um modelo em que o Mps1 é alvo de uma dupla regulação pela Polo. A cinase Polo promove a ativação inicial de Mps1 durante profase. Uma vez que em *Drosophila* a localização de Mps1 depende da sua atividade catalítica, esta ativação é importante para permitir o recrutamento inicial de Mps1 para os cinetocoros que por sua vez é necessário para estabelecer um SAC potente. A ativação de Mps1 por sua vez expõe o seu N-terminal que é fosforilado por Polo para inibir a atividade de Mps1 e promover a sua remoção dos cinetocoros. Este mecanismo confere sensibilidade ao SAC, permitindo o seu imediato silenciamento após a ligação de todos os cinetocoros ao fuso mitótico.

Palavras-chave: Polo, Mps1, SAC, Cinetocoro, Mitose, Regulação.

Table of Contents

Table of Figures

List of Tables

List of Abbreviations

APC/C	Anaphase Promoting Complex/Cyclosome
ATP	Adenosine triphosphate
bp	base pairs
BSA	Bovine Serum Albumin
Bub	Budding uninhibited by benzimidazole
BubR1	Bub1-related protein kinase
C-Mad2	Closed Mad2
C. elegans	*Caenorhabditis elegans*
Cdc	Cell division cycle
Cdh	Cdc20 homolog
Cdk	Cyclin-dependent kinase
cDNA	complementary DNA
CDS	Coding sequence
CID	Centromere Identifier
D box	Destruction box
DAPI	4,6-diamidino-2-phenylindole
DNA	Deoxyribonuclein acid
ds	double stranded
DTT	Dithiothreitol
ECL	Enhanced Chemiluminescence
EDTA	Ethylenediaminetetraacetic acid
EGFP	Enhanced Green Fluorescent Protein
EGTA	Ethyleneglycoltetraacetic acid
FBS	Fetal Bovine Serum
FRAP	Fluorescence Recovery After Photobleaching
Hec1	Highly expressed in cancer 1
HEPES	4-(2-hydroxyethyl)-1-piperazineethanesulfonic acid
HRP	Horseradish Peroxidase
IB	Immunoblotting
IF	Immunofluorescence

IP	Immunprecipitation
KD	kinase-death
KEN box	KENxxxN/D motif
KMN	Knl-1/Mis12 complex/Ndc80 complex
Knl-1	Kinetochore null-1
LB	Luria Bertani medium
Mad	Mitotic arrest deficient
MCC	Mitotic Checkpoint Complex
mCherry	Monomer red fluorescent protein
MOPS	3-(N-Morpholino)propanesulfonic acid
Mps1	Monopolar spindle 1
$Mps1^{4D}$	Mps1 mutated on Threonine 185, 197 260 and Serine 262 to Aspartate
$Mps1^{4A}$	Mps1 mutated on Threonine 185, 197 260 and Serine 262 to Alanine
$Mps1^{T490Ph}$	Mps1 phosphorylated on Threonine 490
mRNA	messenger RNA
Ndc80	Nuclear division cycle 80
NEB	Nuclear Envelope Breakdown
NTE	N-terminal extension
Nuf2	Nuclear filament-containing protein 2
O-Mad2	Open Mad2
Ph	Phosphorylated
PBS	Phosphate-buffered saline
PBST	PBS 0.05% Tween20
PBSTF	PBS 0.05% Tween20 10% FBS
PCR	Polymerase Chain Reaction
PBD	Polo Box Domain
PIPES	Piperazine-1,4-bis(2-ethanesulfonic acid)
Plk1	Polo-like kinase 1
$Polo^{T182D}$	Polo mutated on Threonine 182 to Aspartate
RNA	Ribonucleic acid
RNAi	RNA interference
ROI	Region of interest
RZZ	Rough Deal/Zeste White 10/Zwilch
S2 cells	*Drosophila* Schneider cells

SAC	Spindle Assembly Checkpoint
SDS	Sodium dodecyl sulfate
SDS-PAGE	Sodium dodecyl sulfate polyacrylamide gel electrophoresis
SPB	Spindle Pole Body
TPR	Tetratricopeptide domain
UTR	Untranslated region
WB	Western blot
WT	wild-type
Zw10	Zeste White 10

CHAPTER 1

INTRODUCTION

1.1. Mitosis overview

Growth and regeneration of tissues depend on cell division. This process can either occur symmetrically, to increase the number of a specific cell type, or asymmetrically, to generate specialized cells, but always involves the equal separation of the genetic material to two daughter cells. The term mitosis, which refers to the actual process of cell division in eukaryotes, was coined in the 1880s, by Walther Flemming, upon observing what looked like threads in dividing cells (from the Greek word *mitos*; Mitchison and Salmon, 2001). The sequence of processes, starting with a signal to begin cell division and ending in the actual division of the cell, is known as the cell cycle. Before two new daughter cells can be generated, mother cells need to have duplicated their DNA and organelles, processes taking place in the phases preceding the mitotic phase. These phases are called the G1, S and G2 phases of the cell cycle, collectively termed interphase, and are sequentially initiated due to the activity of several Cyclin-dependent kinases (Cdks) in complex with Cyclins.

The DNA of eukaryotic cells is orderly folded and packed into chromosomes in the nucleus of the cell. Each duplicated chromosome remains associated with its sister chromatid from the moment of replication in S phase until the end of mitosis. Progression through mitosis encompasses distinct morphological stages that ensure the proper distribution of sister chromatids to the new daughter cells (Figure 1.1.1). After initiation of DNA condensation during ***prophase***, increased levels of Cdk1-Cyclin B signal the irreversible entry into mitosis and lead to nuclear envelope breakdown (NEB; Gavet and Pines, 2010; Virshup and Kaldis, 2010). During ***prometaphase***, microtubules of the mitotic spindle interact with chromosomes through kinetochores - specialized multi-protein structures assembled on centromeric DNA (Cheeseman and Desai, 2008). Kinetochore-microtubule attachment favors the gradual alignment of chromosomes to the equator of the mitotic spindle, with each kinetochore from a pair attached to microtubules from opposite poles (***metaphase***). This conformation is known as bi-orientation and ensures the correct segregation of chromosomes to the new daughter cells. At this point, the anaphase-promoting complex/cyclosome (APC/C) is activated by Cell division cycle 20 (Cdc20). The APC/C is an E3 ubiquitin ligase, which targets several mitotic substrates for degradation by the 26S proteasome, among which Cyclin B and Securin (Hagting et al., 2002; King et al., 1995; Pines, 2011). Degradation of Cyclin B leads to Cdk1 inactivation, which is essential for mitotic exit (Wolf et al., 2006). Securin is a stoichiometric inhibitor of

Separase, a protease, which in turn cleaves the Cohesin complex holding sister chromatids together. Its removal therefore allows sister chromatid separation and ***anaphase*** onset. During ***telophase*** chromosomes decondense and nuclear envelope reforms around them, giving rise to two separate daughter nuclei. At the end of cell division a contractile ring forms midway between the two new nuclei and, upon constriction, pinches the cell in two at cytokinesis.

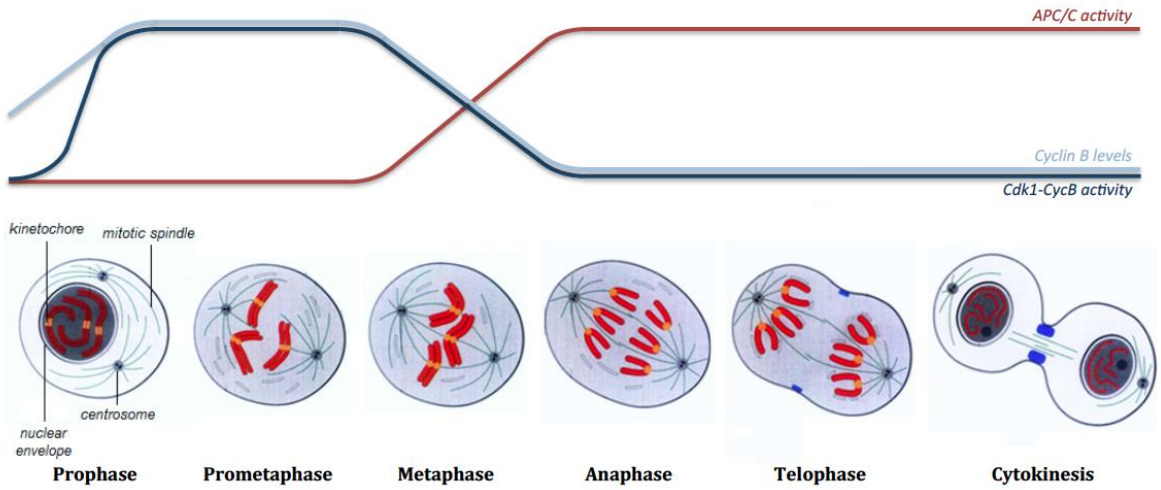

Figure 1.1.1 - Mitotic stages. During prophase DNA condensation becomes visible and centrosomes separate. Rising Cyclin B levels activate Cdk1, which drives mitotic progression. NEB marks the beginning of prometaphase and allows bipolar spindle formation. Upon correct kinetochore-microtubule attachment, chromosomes align at the metaphase plate. At this point APC/C activity rises, leading to Cdk1-CycB inactivation and beginning of anaphase. After segregation of sister chromatids to opposite poles, nuclear envelope reforms during telophase. The resulting two daughter cells emerge at cytokinesis after constriction of a contractile ring, which separates their cytoplasmic content (adpated from Morgan, 2007).

1.2. The spindle assembly checkpoint

Each time a cell divides, it must duplicate the entire genome and distribute one copy of each chromosome into each daughter cell. Aneuploidy arises as a result of errors in chromosome partitioning during mitosis and has for long been associated with development defects and cancer. Millions of cell divisions occur every minute in the adult human body and therefore the maintenance of genomic content requires each chromosome to be segregated with high fidelity during every division.

To ensure the accuracy of chromosome segregation, eukaryotic cells evolved the ability to coordinate kinetochore attachment status with a feedback mechanism known as

Spindle Assembly Checkpoint (SAC), a biochemical pathway that restrains the irreversible transition into anaphase until all kinetochores are correctly attached to the mitotic spindle (Vleugel et al., 2012). Seminal work by Rieder and colleagues demonstrated that a single unattached kinetochore was sufficient to prevent anaphase onset (Rieder et al., 1995; Rieder et al., 1994). This indicates that the SAC operates as surveillance mechanism monitoring kinetochore-microtubule attachments and that unattached kinetochores serve as catalytic platforms for the production of a robust diffusive “wait anaphase signal” (Figure 1.2.1) (Lara-Gonzalez et al., 2012).

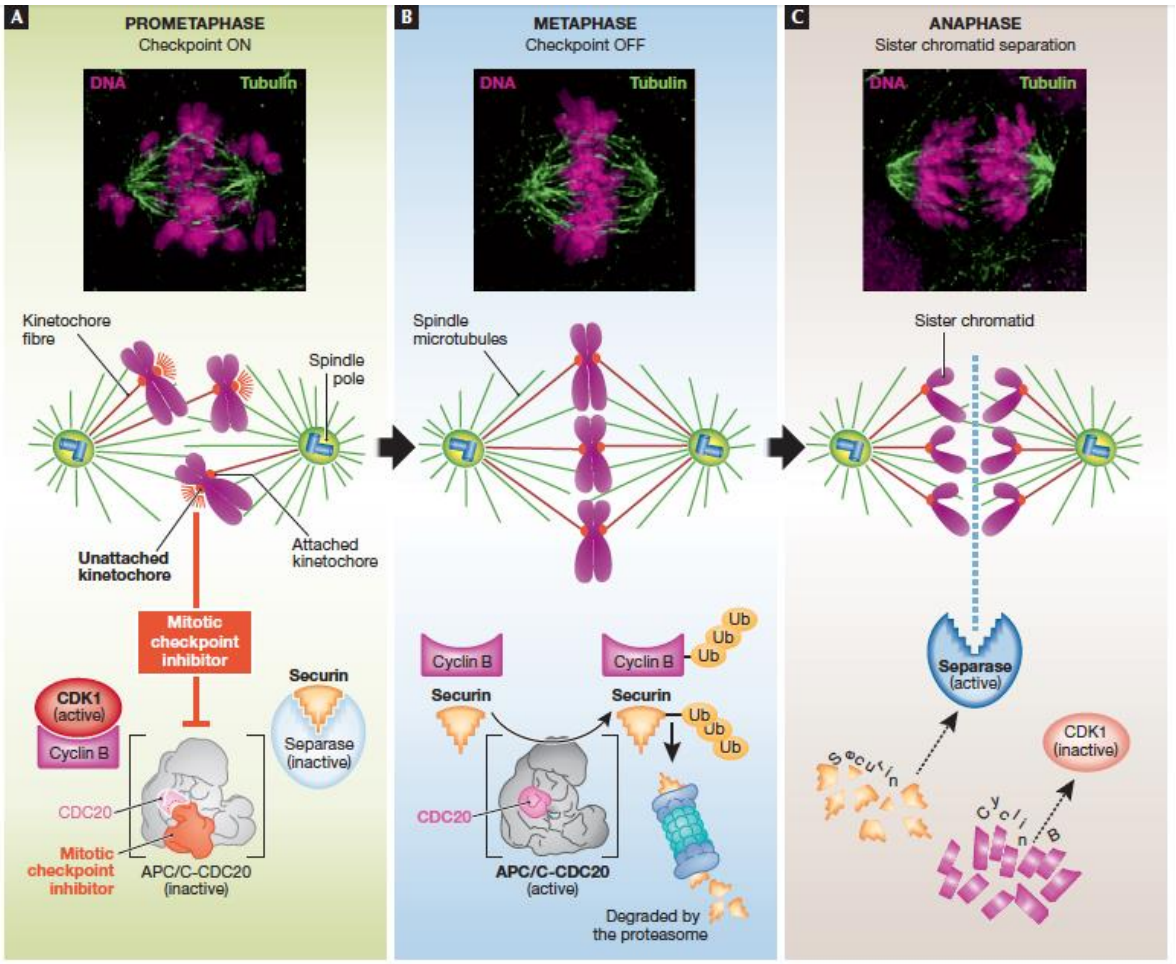

Figure 1.2.1 - The Spindle Assembly Checkpoint: a surveillance mechanism to ensure accurate chromosome segregation. (A) To guard against chromosome missegregation and aneuploidy, cells have evolved a surveillance pathway known as the mitotic checkpoint that halts progression into anaphase until all of the kinetochores have attached to the microtubules of the mitotic spindle. Unattached kinetochores release a diffusible signal that inhibits ubiquitination of Cyclin B and Securin by the APC/C bound to its activator Cdc20. (B) At metaphase, when all kinetochores are correctly attached to microtubules of the spindle, the mitotic checkpoint is silenced and APC/Cdc20 ubiquitinates Securin and Cyclin B, thereby targeting them for destruction by the 26S proteasome. (C) Destruction of Securin liberates separase, which promotes loss of

sister chromatid cohesion, and Cyclin B1 destruction inactivates Cdk1 thereby promoting mitotic exit (from Holland and Cleveland, 2012).

The target of the SAC is the APC/C. The co-activators Cdc20 and Cdh1 are used by the APC/C to recognize two targeting motifs on substrates, a Lys-Glu-Asn (KEN)-box and Arg-x-x-Leu (RxxL)-box (also known as Destruction (D)-box), respectively. Activity of the APC/C towards Securin and Cyclin B is prevented by its interaction with the Mitotic Checkpoint Complex (MCC), a four-protein complex, consisting of Mad2, Bub3, BubR1 and Cdc20, whose assembly is promoted by unattached kinetochores (Lara-Gonzalez et al., 2012). Models for SAC molecular framework (Figure 1.2.2) suggest that Mad1/Mad2 heterotetramers associate with unattached kinetochores and catalyze the conformational activation of cytosolic open Mad2 (O-Mad2) to a closed conformer (C-Mad2) (De Antoni et al., 2005), which facilitates subsequent binding to Cdc20 (Mapelli et al., 2007; Simonetta et al., 2009). The C-Mad2-Cdc20 interaction primes Cdc20 to bind BubR1, which is, then, able to engage Cdc20 through its N-terminal KEN box (Davenport et al., 2006; Kulukian et al., 2009; Malureanu et al., 2009; Sczaniecka et al., 2008). It remains unclear, how C-Mad2-Cdc20 and BubR1-Bub3 intersect to form the MCC. Recent work has shown that Mps1-dependent phosphorylation of BubR1 might play an important role in promoting its binding to Cdc20 and allow the assembly of the final MCC (Conde et al., 2013a).

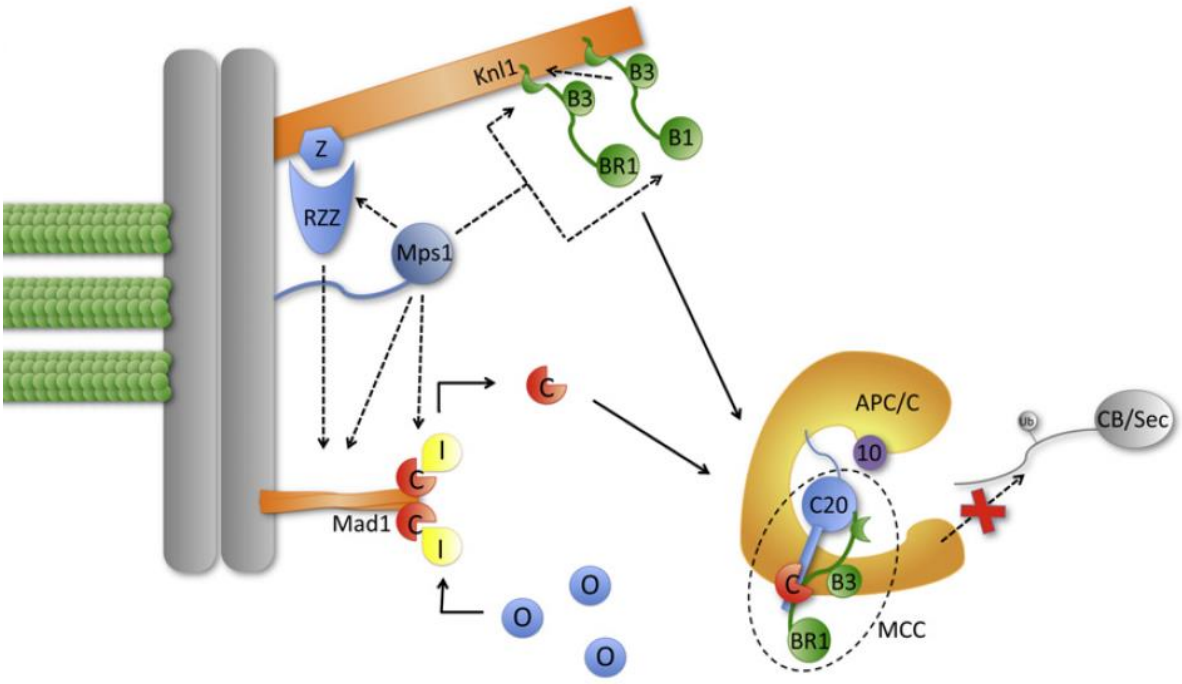

Figure 1.2.2 - MCC assembly and APC/C inhibition. (A) Unattached kinetochores recruit Mad1, Bub1 (B1), BubR1/Mad3 (BR1), Bub3 (B3), and the RZZ complex (RZZ) either directly or indirectly via the scaffold Knl1/Zwint-1 (Z). The combined actions of these proteins and protein complexes promote conversion of O-Mad2 (O) into C-Mad2 (C) after its dimerization with Mad1-bound C-Mad2. Soluble C-Mad2 and BubR1/Mad3 then bind the APC/C coactivator Cdc20 (C20), blocking its substrate binding sites and repositioning Cdc20 away from the APC/C subunit Apc10. As a result, APC/C-mediated ubiquitination (Ub) of Cyclin B (CB) and Securin (Sec) are inhibited, maintaining sister chromatid cohesion and a mitotic state. Various steps in these processes are under control of Mps1 (from Vleugel et al., 2012).

1.3. Mitotic kinases in the spindle assembly checkpoint

Protein kinases are critical regulators of cell division (Figure 1.3.1). Apart from Cdks, which are considered the master regulators, a set of additional conserved kinases control progression through mitosis, including Polo, Aurora, Bub, NEK/NimA and Mps1 kinases. Because of the widely conserved nature of their functions in mitosis, these are collectively called mitotic kinases. Reversible protein phosphorylation has long been accredited as a regulatory mechanism of the SAC. There is solid evidence that several proteins related to SAC function are phosphorylated during mitosis, including Mad1, Mad2 and BubR1 (Hardwick and Murray, 1995; Huang et al., 2008; Zich et al., 2012). Nevertheless, the relevance of most phosphorylation events remains elusive and

knowledge of how several mitotic kinases act in concert within the signaling pathway to orchestrate SAC function is still emerging.

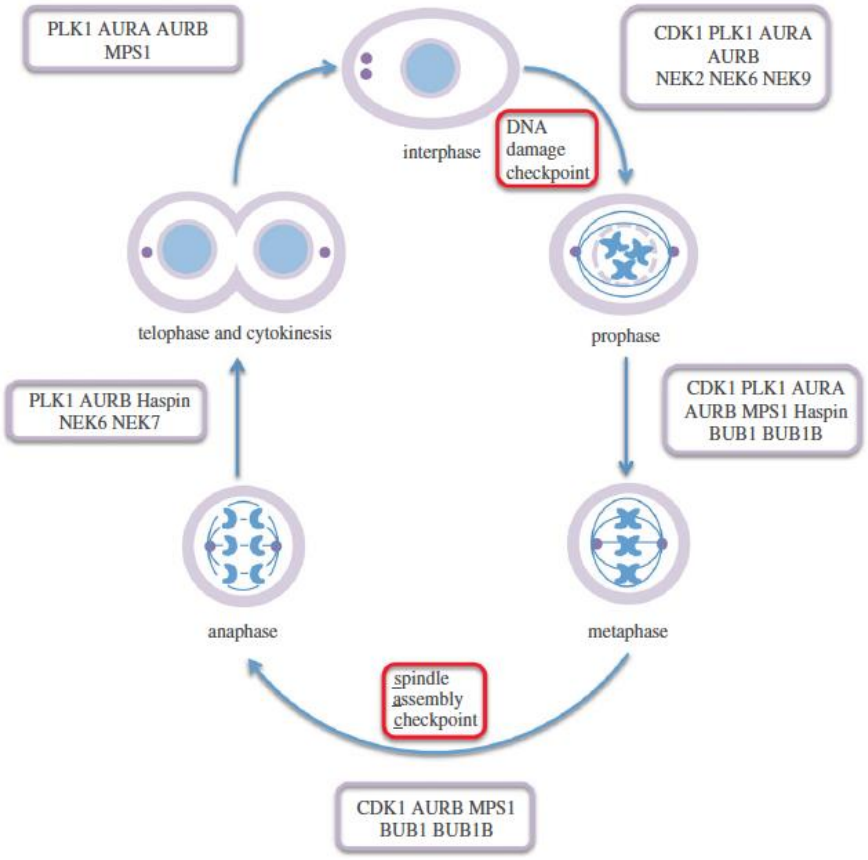

Figure 1.3.1 - Protein kinases regulate cell cycle progression. An illustration depicting the involvement of several mitotic kinases during mitotic entry, mitotic progression and mitotic exit. Many of the kinases play roles in multiple stages of mitosis (from Bayliss et al., 2012)

1.3.1. Mps1 kinase

1.3.1.1. Mps1 overview

Monopolar spindle 1 (Mps1) is a serine-threonine kinase present in eukaryotes from yeast to humans, the nematode *C. elegans* being a notable exception. Originally identified as a kinase essential for spindle pole body (SPB) duplication in budding yeast, Mps1 was soon found to be a critical regulator of SAC signalling (Liu and Winey, 2012). While its role in the SAC appears to be both universally conserved and essential in most

organisms, conservation of its originally described function in spindle pole duplication has proven controversial (Pike and Fisk, 2011).

Mps1 is required for SAC function by acting at multiple points along the signalling pathway. Mps1 checkpoint function is attributed to its upstream role in the recruitment of Mad1, Mad2, BubR1, Bub1 and Bub3 to unattached kinetochores (Lan and Cleveland, 2010). Its activity was also shown to be required for Mad2 conformational activation by maintaining the recruitment of O-Mad2 to kinetochore-associated Mad1-Mad2 heterotetramers (Hewitt et al., 2010; Zich et al., 2012) and for the formation or stability of APC/C inhibitory complexes (Maciejowski et al., 2010). Although the molecular mechanisms by which Mps1 orchestrates Mad1 and Mad2 kinetochore localization and function remain unclear, important insights were recently provided regarding the role of Mps1 in the recruitment of Bub proteins to unattached kinetochores. In fungi and in human cells, Mps1 promotes Bub1/Bub3 and BubR1/Bub3 kinetochore localization through phosphorylation of Knl1/Spc105/Spc7 (London et al., 2012; Shepperd et al., 2012; Yamagishi et al., 2012). Knl1 contains an array of sequence variants of Met–Glu–Leu–Thr (MELT) motifs that turn into high-affinity binding sites for Bub3 after phosphorylation by Mps1 kinase. The selectivity for phosphorylated MELT-like motifs (MELTph) is explained by ionic interactions between basic residues of Bub3 and the acidic phosphate group, which are potentiated by Bub3-associated Bub1 (Primorac et al., 2013). Interestingly, *Drosophila* Spc105/Knl1 has specific MELT-like motifs that lack the phosphorylatable threonine, hence making Mps1 dispensable for kinetochore recruitment of Bub1, BubR1 or Bub3 in flies (Conde et al., 2013b). This uncovered a direct role of Mps1 in controlling MCC assembly in *Drosophila*. Mps1 was shown to promote BubR1 phosphorylation resulting in the formation of the 3F3/2 phosphoepitope at unattached/tensionless kinetochores. This facilitates the association of Cdc20 with BubR1 at kinetochores, thereby increasing the concentration of the BubR1-Cdc20 complex at the site where C-Mad2 is generated, hence allowing efficient MCC assembly (Conde et al., 2013a).

1.3.1.2. Regulation of Mps1

To accomplish a myriad of functions, Mps1 must be exquisitely regulated. Mps1 kinases are expressed at low levels, and the most important regulatory mechanisms operate via phosphorylation and degradation. Mps1 abundance throughout the cell cycle is controlled at the transcriptional level by the E2F family of transcription factors. Correlating

with functions of Mps1 specifically during mitosis, Mps1 transcription is repressed in interphase and upregulated in G2 and mitosis (Liu and Winey, 2012). Mps1 expression peaks in mitosis and declines when cells enter anaphase. After completing its mitotic functions, Mps1 is targeted for degradation at mitotic exit by both Cdc20- and Cdh1-associated APC/C complexes ensuring low cytoplasmic levels of Mps1 in G1 (Pike and Fisk, 2011).

In accordance with its upstream role in SAC signalling, Mps1 is recruited to unattached kinetochores. Kinetochore localization of Mps1 is thought to favor its dimerization, hence promoting Mps1 trans-autophosphorylation on the T-loop, rendering the kinase fully active, which was shown to be required for efficient SAC function (Hewitt et al., 2010; Kang et al., 2007; Santaguida et al., 2010). Nevertheless, the mechanism controlling Mps1 association with kinetochores had remained elusive. Several studies have shown that Aurora B kinase and the outer-kinetochore protein Ndc80 cooperate to promote rapid accumulation and activation of Mps1 at kinetochores (Conde et al., 2013a; Santaguida et al., 2011; Saurin et al., 2011). The N-terminal 301 amino acids of human Mps1 was shown to be sufficient and necessary to direct Mps1 kinetochore localization (Liu et al., 2003; Stucke et al., 2004) and important mechanistic insights were recently provided by the work of Nijenhuis and colleagues showing that the recruitment human Mps1 to kinetochores depends on the calponin homology domain of Hec1/Ndc80 and on a Mps1 N-terminal localization module harboring a 60 amino acids N-terminal extension (NTE) and a tetratricopeptide (TPR) domain (Nijenhuis et al., 2013). The authors showed that the predominant kinetochore binding activity resides within the NTE and that deletion of the TPR domain renders Mps1 recruitment insensitive to Aurora B inhibition (Nijenhuis et al., 2013). It is therefore tempting to envisage a model for regulation of Mps1 kinetochore recruitment in which the NTE interacts with the TPR domain inhibiting both NTE- and TPR-mediated kinetochore binding. Aurora B activity relieves the TPR-inhibitory constraint on Mps1 localization by promoting the release of the interaction rendering both the NTE and TPR available to mediate kinetochore binding. Interestingly, Aurora B does not seem to directly phosphorylate Mps1 in its N-terminal region indicating that the control exerted over the TPR domain and, therefore, over Mps1 localization is likely indirect. Intriguingly, and contrasting with the human orthologue, no evident TPR domain seems to be present on the N-terminal region of *Drosophila* Mps1 and its kinetochore recruitment was shown to be mediated by its C-terminal kinase domain (Althoff et al., 2012).

Mps1 dynamically exchanges on unattached kinetochores and its kinase activity has been implicated in the control of its kinetochore localization with some puzzling disagreements. Phosphodefective mutations of nine autophosphorylation sites in the N-terminal of human Mps1 caused a significant decrease in kinetochore targeting of Mps1 in SW480 cells (Xu et al., 2009). Consistent with this observation, a kinase-dead version of Mps1 expressed in SW480 cells exhibited reduced kinetochore recruitment upon depletion of endogenous Mps1 (Xu et al., 2009). Likewise, inhibition of endogenous Mps1 in US20S cells with the inhibitor NMS-P715 led to reduction of Mps1 levels at unattached kinetochores (Colombo et al., 2010). On the other hand, other studies showed that inhibition of Mps1 activity with AZ3146 or Mps1-IN-1 increases its half-time of recovery at unattached kinetochores and causes an increase of Mps1 levels at these sites indicating that Mps1 activity promotes its own release from kinetochores (Hewitt et al., 2010; Jelluma et al., 2010). At present, the reason for the observed divergences is not fully understood but it is plausible that it might reflect differences on the cell type, degree of inhibition and experimental conditions. To evaluate whether the kinase activity is required for the kinetochore localization of *Drosophila* Mps1, Althoff and colleagues expressed a kinase-dead version of Mps1 in $Mps1^{aldB4}$ mutant embryos (Althoff et al., 2012). The mutation results in a premature stop after the first 47 amino acids (Page et al., 2007) hence allowing the authors to assess kinetochore recruitment of the catalytic inactive Mps1 without the interference of endogenous Mps1. Under these conditions, $Mps1^{KD}$ levels at prometaphase kinetochores were dramatically reduced when compared with $Mps1^{WT}$ expressed analogously; clearly indicating that Mps1 kinase activity is required for its kinetochore localization in *Drosophila* (Althoff et al., 2012).

1.3.2. Polo kinase

1.3.2.1. Polo overview

Genetic screens led to the discovery of the first members of the Polo-like kinase (Plk), Cdc5 and Polo, in budding yeast and *Drosophila* respectively (Hartwell et al., 1973; Sunkel and Glover, 1988). Although the original mutant phenotypes were characterized by the presence of abnormal spindles (Sunkel and Glover, 1988), subsequent studies of different mutant alleles showed that Plks orchestrate multiple processes during mitosis (Zitouni et al., 2014).

The role of Polo kinases in SAC signalling remains elusive and controversial. Human Plk1 was initially linked to SAC function through the generation of the 3F3/2 phosphoepitope at kinetochores of chromosomes that are not under tension (Ahonen et al., 2005). However, the relevance of this phosphoepitope for SAC signalling has remained unclear. Subsequent work revealed that phosphorylation of BubR1 by Plx1 generated the 3F3/2 phosphoepitope and was required for SAC arrest in *Xenopus* egg extracts (Wong and Fang, 2005), opposing to data obtained with human cells (Lenart et al., 2007; Sumara et al., 2004). In this system, Plk1-mediated phosphorylation of BubR1 was shown to be important rather for the stability of kinetochore-microtubule attachments (Elowe et al., 2007; Matsumura et al., 2007). Moreover, several reports have shown that Plk1 inhibition or RNAi-mediated silencing causes a SAC-dependent prometaphase arrest with accumulation of Mad2 and BubR1 at kinetochores (Lenart et al., 2007; Petronczki et al., 2008; Sumara et al., 2004). This contrasts with previous results showing a significant decrease of Mad2 and Cdc20 accumulation at unattached kinetochores upon inhibition of Plk1 expression (Ahonen et al., 2005), as well as with its role in Mad1 phosphorylation to allow its localization at unattached kinetochores and consequently Mad2 accumulation and SAC activity (Chi et al., 2008).

Recent results obtained in *Drosophila* provided important new insights into this controversy (Conde et al., 2013b). Loss of Polo activity in S2 cells results in a mitotic arrest that was shown to be SAC independent. Interestingly, Polo depletion severely reduced APC/C mediated ubiquitination of Cyclin B in SAC impaired cells suggesting that Polo is required for mitotic exit possibly by promoting APC/C activation (Conde et al., 2013b). This requirement masks a role for Polo in SAC signaling, clearly revealed by significantly decreased levels of MCC and failure to recruit Mad2 to unattached kinetochores in the absence of Polo activity (Conde et al., 2013a). Polo contributes for SAC function in flies at least through two pathways that converge to ensure prompt and efficient Mps1 recruitment to unattached kinetochores: (i) Polo promotes proper loading of Mps1 kinetochore receptor Ndc80 (Conde et al., 2013a) and (ii) controls Aurora B centromeric localization and activity (Conde et al., 2013a; Moutinho-Santos et al., 2012), which synergizes with Ndc80 to potentiate Mps1 kinetochore localization in early prometaphase required for robust SAC signaling. Interestingly, expression of a constitutively active form of Polo revealed that Polo might also directly regulate Mps1 kinetochore recruitment by a mechanism that remains unclear (Conde et al., 2013a; Conde et al., 2013b).

1.3.2.2. Regulation of Polo

Polo kinases have an amino-terminal serine-threonine catalytic domain and a carboxyl-terminal region containing two conserved Polo boxes that compose the characteristic Polo Box Domain (PBD) which regulates in part the kinase activity, confers substrate specificity and controls subcellular localization. Polo kinases are additionally controlled by phosphorylation, proteolysis and transcription, depending on the biological context.

The expression of Plks is tightly regulated in time at both mRNA and protein levels, being low in interphase and high in mitosis (Zitouni et al., 2014). Expression of the Plk1 gene is under the control of various transcriptional repressors in G1 and transcriptional activators in G2. Within the Plk1 promoter, CDE–CHR sequences are involved in repressing Plk1 transcription during G1, in coordination with the cellular tumor antigen p53 and/or p21 (Zitouni et al., 2014). In addition, in humans and *Drosophila*, RB and the E2F family of transcription factors function together to repress Plk1 and Polo gene expression (Archambault and Glover, 2009). During G2, the multisubunit DREAM complex promotes Polo kinases transcription in animals and yeasts through the transcription factor FOXM1 (Zitouni et al., 2014). Plks are subjected to ubiquitin-dependent proteolysis by the proteasome. Degradation is initiated during anaphase triggered by APC/C-Cdh1 that recognizes a D-box conserved in Polo orthologues of higher eukaryotes. Paradoxically, PLK activity is required for cytokinesis and Cenp-A deposition at centromeres and has been found to be present at centromeres in G1 (McKinley and Cheeseman, 2014), suggesting a localized degradation of Plks.

In addition to being regulated at the level of expression, the subcellular localization of Plks is also dynamically regulated, which contributes to fine-tune the activity of these proteins and is crucial for their multiple functions in mitosis. Critical for the spatial regulation of Polo activity is the PBD. The two Polo boxes form a binding pocket that interacts with phosphopeptides Ser-[pSer/pThr]-[Pro/X] previously phosphorylated by Pro-directed kinases like Cdk1, MAPKs or Plk itself. The interaction between Plks and their targets is hence modulated in space and time by the activity of specific kinases (Archambault and Glover, 2009).

The PBD regulates Plk kinase activity by binding to the kinase domain in a conformation that mutually inhibits its activity. Structural studies revealed that the kinase domain is inhibited in three ways: (i) by the PBD itself, which reduces the flexibility of the

kinase domain hinge region; (ii) by the interdomain linker, which links the kinase domain with the PBD and sequesters the T-loop and (iii) by binding of the PBD to Map205 protein, which stabilizes the autoinhibited state and also sequesters the kinase from its substrates (Zitouni et al., 2014).

Plks activity increases at the G2/M transition, reaching a maximum during mitosis (Bruinsma et al., 2012). Phosphopeptide binding and/or phosphorylation of the conserved Thr^{210} in the T-loop (Thr^{182} in *Drosophila*) contribute to coordinate spatiotemporal Polo activation. Aurora A was shown to phosphorylate Plk1 on Thr^{210} before mitotic entry (Macurek et al., 2008; Seki et al., 2008; van de Weerdt et al., 2005), whereas Aurora B seems to phosphorylate the same residue during mitosis (Carmena et al., 2012). This activating phosphorylation is postulated to disrupt the intramolecular interaction between the kinase domain and the PBD that inhibits the functions of both domains (Jang et al., 2002; Lowery et al., 2005).

1.4. Objectives

Maintenance of genomic stability during eukaryotic cell division relies on the SAC that operates as a surveillance mechanism to restrain anaphase onset until all chromosomes are correctly attached to microtubules from opposite spindle poles. A single unattached kinetochore generates a signal strong enough to inhibit APC/C activity and consequently halt mitotic progression. Remarkably, anaphase takes place swiftly after all kinetochores stably attach to spindle microtubules, revealing that the SAC is not only extremely robust, but also highly responsive allowing prompt SAC silencing. How the SAC encompasses simultaneously both features remains unclear. Mps1 kinase is a key SAC regulator that acts at several levels along the SAC pathway to promote MCC assembly. However, the mechanisms controlling its kinetochore recruitment, activation and inactivation remain elusive.

The aim of this thesis is to uncover novel molecular mechanisms underlying Mps1 regulation and their relevance to establish SAC robustness and responsiveness. Using *Drosophila* as a model we provide evidence that Polo exerts a dual regulation over Mps1 activity. Polo promotes Mps1 activation at the nuclear envelope/pore and its subsequent nuclear import during prophase. This initial Mps1 activation is required to direct auto-phosphorylation dependent Mps1 recruitment to prometaphase kinetochores, hence

establishing SAC robustness. At kinetochores, fully active Mps1 is phosphorylated by Polo in its N-terminal region. This event negatively regulates Mps1 activity and promotes the kinase prompt dissociation from kinetochores. This mechanism contributes to Mps1 dynamic behavior at kinetochores during prometaphase and allows fast SAC silencing upon biorientation, hereby providing SAC responsiveness.

CHAPTER 2

MATERIALS AND METHODS

2.1. Competent TOP10 cells generation and transformation by heat chock

To produce competent TOP10 cells (Invitrogen), 500 mL of LB medium were inoculated with 5 mL of a starting culture grown overnight and incubated at 37ºC. After reaching an OD_{595} of roughly 0.5, cells were cooled down on ice for 15 minutes and collected through centrifugation for 10 minutes at 4500 rpm and 4ºC. Cell pellet was ressuspended in 30 mL of sterile Tfb I (100 mM RbCl, 50 mM $MnCl_2$-$4H_2O$, 30 mM potassium acetate, 10 mM $CaCl_2$-$2H_2O$, 15% glycerol, prepared in deionized water) and incubated on ice for another 15 min. Afterwards, cells were centrifuged for 5 minutes at 4000 rpm and 4ºC and ressuspended in 6 mL of sterile Tfb II (0.2 M MOPS pH 6.5, 10 mM RbCl, 70 mM $CaCl_2$-$2H_2O$, 15% glycerol, prepared in deionized water). Aliquots were frozen in dry ice and stored at -80ºC.

To transform competent TOP10 cells, 50 µL aliquots were defrosted on ice for a short period and incubated for 20 minutes with at least 10-15 ng of the intended vector, ligation reaction or vector-containing Whatman card. Transformation was induced through heat shock for 45-60 seconds at 42ºC and after 2 minutes on ice, cells were incubated for one hour at 37ºC with an additional 200 µL of LB medium. To select for transformed bacteria, cells were plated on LB agar supplemented with adequate antibiotics. Ampicillin and kanamycin were used at the respective final concentrations of 100 µg mL^{-1}, 50 µg mL^{-1} Plasmid extractions were done with Fast-n-Easy Plasmid Mini-Prep Kit (Jena Bioscience GmbH) according the manufacturer's instructions.

2.2. RNA interference (RNAi) synthesis

To deplete Polo and BubR1 from *Drosophila* S2 cells, double stranded (ds)RNA was synthesized, targeting *Polo* and *BubR1* 5'UTR and 5'end of the coding region as previously described (Maia et al., 2007; Moutinho-Santos et al., 2012). For RNAi synthesis, *Polo* (LD11851) and *BubR1* (LD23835) cDNA fragments containing the 5'UTR region and the 5'end of the coding region were purchased from Berkeley *Drosophila* Genome Project DGRC gold collection and cloned into both pSPT18 and pSPT19 expression vectors (Roche). RNAi was synthesized using a T7 Megascript kit (Ambion)

following the manufacturer's instructions. The obtained RNA was heated for 5 min to 96ºC, to denature secondary structures, and gradually cooled down (2ºC every minute) in order to allow formation of dsRNA duplex. The integrity dsRNAi duplexes was evaluated by 1% agarose gel electrophoresis and the concentration and purity degree determined measuring the absorbance in a nanodrop (Nanodrop Spectrophotometer ND-1000).

2.3. S2 cell culture, RNAi-mediated depletion and drug treatment

Drosophila S2 cells were cultured at 25°C in Schneider's medium (Gibco, BRL) supplemented with 10% fetal bovine serum (FBS). For each depletion, 10^6 S2 cells/mL of Schneider's medium (Gibco, BRL) were plated in six (0.5 mL) or twelve-well plates (1 mL) and 30 µg of the respective dsRNAi was added per mL of media. After one hour at 25°C, cells were supplemented with Schneider's medium (Gibco, BRL) with 10% FBS to a final concentration of 0.33 cells mL^{-1}. The incubation period was 120 hours for BubR1 (Maia et al., 2007) and 72 hours for Polo (Moutinho-Santos et al., 2012). At the selected time points, cells were collected and processed for immunofluorescence, time-lapse microscopy, immunoprecipitation or immunoblotting. Protein depletion was monitored through Western blotting or immunofluorescence analysis.

When required, cells were subjected to several drug treatments before being collected and processed. In order to depolymeraze microtubules, cells were incubated with 30 µM colchicine (Sigma) for selected time periods. To prevent mitotic exit in a checkpoint independent manner, cells were incubated for 1-3 hours with proteasome inhibitor MG132 (Calbiochem) at a final concentration of 20 µM. Polo activity was inhibited using BI2537 (Boehringer Ingelheim) at a final concentration of 100 nM.

To induce expression of EGFP-Mps1 transgenes under regulation of a metallothionein promoter, $CuSO_4$ was added to cultures at a final concentration of 50 µM 12 hours before analysis. Expression of $Polo^{T182D}$-GFP $Polo^{WT}$-GFP promoted by heat shock was induced through incubation at 37°C 6 hours prior to processing of cells.

2.4. Constructs

To generate Polo-EGFP (Polo^{T182D}-EGFP), a 300 bp DNA fragment containing the mutation for Polo^{T182D} was generated by gene synthesis from GeneArt® Life technology (Invitrogen) and replaced the corresponding region of wild-type Polo cDNA previously cloned in the pGEMTeasy vector. Polo full coding region was then amplified by PCR with specific primers suitable for Gateway cloning system (Invitrogen). Expression vector pH-WG-Polo^{T182D} was generated by Gateway recombination (Invitrogen) of pENTR-Polo^{T182D} clone into pH-WG (heat-shock inducible promoter, C-terminal EGFP tag) destination vector. The same strategy was used to obtain pH-WG-Polo^{WT}.

To generate EGFP-Mps1^{WT}, Mps1 coding sequence (CDS) was cloned in frame with N-terminal EGFP under regulation of a metallothionein promoter in the pMT-EGFP-C vector (Invitrogen). Full-length *Mps1* cDNA was purchased from Berkeley Drosophila Genome Project DGRC gold collection (clone LD04521). Mps1 CDS was amplified through PCR reaction using the set of primers indicated in Table 2.4.1, and FideliTaq DNA Polymerase (USB) according to the manufacturer's instructions with 35 cycles of denaturation at 95ºC for 50 seconds, annealing at 55ºC for another 50 seconds and extension at 72ºC for 2 minutes. The resulting Mps1 PCR product and pMT-EGFP-C were digested with XhoI and XmaI restriction enzymes (New England Biolabs) overnight, according to the manufacturer's instructions. After inactivation of the restriction enzymes through incubation at 65ºC for 20 minutes, the PCR product was purified (Agarose Gel Extraction Kit, Jena Bioscience GmbH) and roughly 150 ng were mixed with 50 ng of digested destination vector and incubated with T4 DNA ligase (New England Biolabs) overnight at 16ºC. Afterwards, the ligation reaction was used to transform competent cells. Individual colonies were grown overnight in 5 mL of LB medium supplemented with ampicillin. To identify vectors containing the inserts, at least 400 µL of each culture was harvested and cells ressuspended in 100 µL of cracking buffer (0.1 M NaOH, 0.25% SDS, 0.2% bromophenol blue, 5 mM EDTA pH 8.0, 10% sucrose, prepared in deionized water). After denaturation at 72ºC for 5 minutes, cell content was run in a 1% agarose gel and positive cultures identified through the slower migration of the plasmid. Insertion was confirmed through restriction analysis or PCR and plasmids were sequenced (Eurofins MWG Operon, Germany).

Table 2.4.1 - Mps1 primers. Set of primers used to clone Mps1 into pMT-EGFP-C vector. XhoI and XmaI restriction are underlined.

Forward	5' CCGCTCGAGTGACCACGCCTGTGCCCC 3'
Reverse	5' TCCCCCCGGGTTAATTGCTGTTGGCGGTT 3'

Phosphomimetic and phosphodefective versions of EGFP-Mps1 for putative Polo phosphorylation residues (Thr185, Thr197, Thr260 and Ser262) were generated by site-directed mutagenesis. First, a fragment of $Mps1^{T197D/A}$ was amplified from pMT-EGFP-Mps1 by PCR using Pfu DNA Polymerase (Fermentas) with the set of primers indicated in Table 2.4.2. For the PCR reaction, 18 cycles of denaturation at 98ºC for 10 seconds, annealing at 55ºC for 30 seconds and extension at 72ºC for 3 minutes were performed. Afterwards, 15 µL of $Mps1^{T197D/A}$ PCR product was digested with DpnI restriction enzyme (New England Biolabs) at 37ºC for at least one hour and a half and used to transform competent bacteria. Once obtained, pMT-EGFP-$Mps1^{197D/A}$ was used as template to generate pMT-EGFP-Mps1 DD/AA using the same procedure and the set of primers indicated in Table 2.4.2. Finally, $Mps1^{4D/4A}$ was amplified from pMT-EGFP-$Mps1^{DD/AA}$ by the same protocol described above. To generate EGFP-Mps1Δ150-300, pMT-EGFP-Mps1 was used as a template for a PCR reaction using Pfu DNA Polymerase (Fermentas) with the set of primers indicated in Table 2.4.1. For the PCR reaction, 3 cycles for each annealing temperature (50, 53, 56, 59, 62, 65, 72ºC) were performed. After this, the same procedure described above was performed.

To generate pFastBac-$Mps^{WT/KD}$ for protein expression in the baculovirus/Sf21 system, pMT-EGFP-$Mps1^{WT/KD}$ and pFastBac HT A were digested with EcoRI and XbaI restriction enzymes (New England Biolabs) at 37ºC for 3 hours. A 1414 bp fragment harboring the CDS of $Mps1^{WT/KD}$ was purified (Agarose Gel Extraction Kit, Jena Bioscience GmbH) and roughly 150 ng were mixed with 50 ng of digested destination vector and incubated with T4 DNA ligase (New England Biolabs) for at least 2 hours at 16ºC. The ligation reaction was used to transform competent cells and positive clones were screened and confirmed as positive as described above.

Table 2.4.2 - Mps1 mutants primers. Sets of forward and reverse primers used to generate Mps1 4D/4A and Mps1 Δ150-300.

Mps1 T197D	Forward: 5' – TGAATTACCCTCCACTAGTAAGGACAAGCCGGATG – 3' Reverse: 5' – GGAGGGTAATTCATTACGCAGTG – 3'
Mps1 T197A	Forward: 5' – TGAATTACCCTCCACTAGTAAGGCGAAGCCGG – 3' Reverse: 5' – GGAGGGTAATTCATTACGCAGTG – 3'
Mps1 T185D T197D (DD)	Forward: 5' – CTCCAAGAGACAGAGGACCCACTGCG – 3' Reverse: 5' – CTCTGTCTCTTGGAGTGGGC – 3'
Mps1 T185A T197A (AA)	Forward: 5' – CTCCAAGAGACAGAGGCCCCACTGCG – 3' Reverse: 5' – CTCTGTCTCTTGGAGTGGGC – 3'
Mps1 T185D T197D T260D S262D (4D)	Forward: 5' – CTGTGCGACACCATCGACGAGGACCCGGACATTC – 3' Reverse: 5' – GATGGTGTCGCACAGGGAGAAG – 3'
Mps1 T185A T197A T260A S262A (4A)	Forward: 5' – CTGTGCGACACCATCGCAGAGGCCCCGGACATTC – 3' Reverse: 5' – GATGGTGTCGCACAGGGAGAAG – 3'
Mps1 Δ150-300aa	Forward: 5' – CATCAATTGCAGCAGTCAAGTGGATAATTGTGGAACCAAAG – 3'

2.5. Production of recombinant His6-Mps1$^{WT/KD}$

To generate pFastBac-Mps$^{WT/KD}$ for protein expression in the baculovirus/Sf21 system, pMT-EGFP-Mps1$^{WT/KD}$ and pFastBac HT A were digested with EcoRI and XbaI restriction enzymes (New England Biolabs) at 37ºC for 3 hours. A 1414 bp fragment harboring the CDS of Mps1$^{WT/KD}$ was purified (Agarose Gel Extraction Kit, Jena Bioscience GmbH) and roughly 150 ng were mixed with 50 ng of digested pFastBac HT A and incubated with T4 DNA ligase (New England Biolabs) for at least 2 hours at 16ºC. The ligation reaction was used to transform competent cells and positive clones were screened and confirmed as positive as described above.

The obtained recombinant pFastBac-Mps$^{WT/KD}$ was used to transform by heat-shock DH10EMBacY competent cells in order to generate recombinant bacmid His6-Mps1$^{WT/KD}$. Transformed bacteria were selected on LB agar supplemented with 25 μg mL^{-1} chloramphenicol, at 37ºC for 48 hours. Positive clones were identified by blue/white screening and validated by re-streaking on fresh LB agar plates containing 50 μg mL^{-1} kanamycin, 7 μg mL^{-1} gentamicin, 10 μg mL^{-1} tetracycline, 40 μg mL^{-1} IPTG and 500 μg mL^{-1} X-gal and incubated overnight at 37ºC. Confirmed positive clones were grown overnight at 37ºC in 3 mL of LB medium supplemented with 50 μg mL^{-1} kanamycin, 7 μg mL^{-1} gentamicin and 10 μg mL^{-1} tetracycline to isolate the recombinant bacmid.

DH10EMBacY baculoviral DNA was isolated with QIAprep Spin Miniprep Kit (QIAGEN) and used to transfect 10^6 Sf21 cells in 6-well plate. 48 hours after transfection, the supernatant was collected (V_0) and used to infect Sf21 cell culture Erlenmeyer shaker flasks. Cell cultures in shaker flasks were split every 24 hours until proliferation arrest. Media containing amplified virus (V_1) was removed 48 hours after proliferation arrest and replenished with fresh media (Fitzgerald et al., 2006; Trowitzsch et al., 2010). Protein expression was monitored by YFP fluorescence and confirmed by SDS-PAGE. Cells were harvested 48 hours post infection and lysed in 50 mM TrisHCl pH 7.5, 500 mM NaCl, 10 mM Imidazole. Lysates were sonicated and clarified by centrifugation at 4°C. Recombinant His6-Mps1$^{WT/KD}$ was purified by affinity chromatography in a His-Trap^{TM}-HP nickel-column (Amersham). The protein was eluted with 250 mM Imidazole and dialysed against 20 mM Hepes pH 7.5, 150 mM NaCl, 10 mM $MgCl_2$, 1 mM DTT.

2.6. *Drosophila* S2 cell transfection

Stable transfection of recombinant plasmids into S2 cells was performed using Cellfectin® II reagent, Life technology (Invitrogen). 10^6 *Drosophila* S2 cells were seeded in a six-well plate in 2 mL Schneider's medium (Gibco, BRL) supplemented with 10% FBS. The desired constructs were diluted in 25 µL of Schneider's medium and slowly mixed with 5 µL of Cellfectin reagent previously diluted in 25 µL of Schneider's medium, as well. After incubation at room temperature for one hour cell medium was replaced with 400 µL of fresh Schneider's medium (Gibco, BRL) and the plasmid mix was slowly added. S2 cells were co-transfected with pCoBlast (Invitrogen), which harbors a blasticidin resistance cassette. After 4 hours, the medium was replaced with fresh Schneider's medium supplemented with 10% FBS. Selection with 25 µg mL^{-1} blasticidin was started after a two-day period.

2.7. Immunofluorescence analysis in *Drosophila* S2 cells

For immunofluorescence analysis, 10^5 cells in 120 µL were centrifuged onto slides for 5 min, at 1000 rpm (Cytospin 2, Shandon). Cells were processed for simultaneous

fixation and extraction in 3.7% formaldehyde, 0.5% Triton X-100 (prepared in PBS) for 10 minutes followed by three washing steps in PBS-Tween20 0.05% (PBST) for 5 minutes each. Alternatively, to reveal spindle morphology or cytoplasmic localization of proteins, cells were fixed with 3.7% formaldehyde in PHEM (240 mM PIPES, 100 mM HEPES pH 7.0, 40 mM EGTA and 16 mM $MgSO_4$) for 12 minutes and extracted with PBS, 0.5% Triton X-100 thrice for 5 minutes. With some antibodies an incubation of 14 minutes in 4% paraformaldehyde followed by an extraction in PBS, 0.1% Triton X-100 was preferred. Slides were immediately used or stored at -20°C in PBS 60% glycerol.

Fixed cells were blocked for one hour in 0.05% Tween 20, 10% fetal bovine serum prepared in PBS (PBSTF) and incubated overnight at 4°C with primary antibodies diluted in PBSTF. After three five-minute washes in PBST and a one hour incubation period with fluorescent-labeled secondary antibodies diluted in PBSTF, cells were washed thrice with PBST for 5 minutes again and slides were mounted with Vectashield mounting medium for fluorescence with 1 mg/mL of DAPI (Vector Laboratories, UK). Images were collected in a Leica TCS SP5 II laser scanning confocal microscope (Leica Microsystems, Germany). Data stacks were analyzed using ImageJ 1.46j software (http://rsb.info.nih.gov/ij/).

For immunofluorescence quantification of proteins, the mean pixel intensity obtained from maximum projected raw images acquired with fixed exposure acquisition settings. Kinetochore and nuclear envelope location was defined manually based on CID and megator staining within a specific predefined region of interest (ROI). After subtraction of background intensities, the intensity relative to CID or megator signal was determined and multiple cells averaged.

2.8. Protein extraction from *Drosophila* S2 cells

Drosophila S2 cultured cells were harvested through centrifugation at 5000 rpm for 10 min at 4°C and afterwards washed twice with at least 2 mL PBS supplemented with protease inhibitors (cOmplete Cocktail Tablets, Roche). Cell pellet was ressuspended in lysis buffer (150 mM KCl, 75 mM Hepes pH 7.5, 1.5 mM EGTA, 1.5 mM $MgCl_2$, 15% glycerol, 0.1% NP-40, protease (cOmplete Cocktail Tablets, Roche) and phosphatase inhibitors (Phosphatase Inhibitor Cocktail 3, Sigma-Aldrich) and frozen in liquid nitrogen. After an incubation time of at least 30 min at 4°C, cell lysates were clarified through centrifugation at 8000 rpm and 4°C for 10 min and quantified by Bradford protein assay

(Bio-Rad). Protein extracts were then either used immediately or frozen in liquid nitrogen and stored at -80°C.

2.9. Immunoprecipitation and Immunoblotting

For immunoprecipitation experiments cells were harvested through centrifugation at 5000 rpm for 10 min at 4°C and afterwards washed with 2 mL PBS supplemented with protease inhibitors cocktail (Roche). Cell pellet was resuspended in lysis buffer (150 mM KCl, 7.5 mM Hepes, pH 7.5, 1.5 mM EGTA, 1.5 mM $MgCl_2$, 15% glycerol, 0.1% NP-40, 1× protease inhibitors cocktail (Roche) and 1× phosphatase inhibitors cocktail 3 (Sigma) before disruption through freezing in liquid nitrogen. Cell lysates were then clarified through centrifugation at 8000 rpm for 10 min at 4°C and quantified by Bradford protein assay (Bio-Rad). 1 mg of extract were used for each immunoprecipitation assay. Lysates were pre-cleared through incubation with 20 µL of magnetic bead bound Protein A or G (New England Biolabs) for 1h at 4°C with rotation, in order to reduce non-specific binding. Pre-cleared extracts were incubated at 4ºC overnight with the primary antibodies. Afterwards they were incubated with 50 µL of magnetic bound Protein A or G for 1.5h at 4°C with rotation. The magnetic beads and bound protein fraction were collected and washed 5 times with 1 mL of lysis buffer. Finally the magnetic beads and bound protein were resuspended in 20 µL of 2x Laemmli sample buffer (4% SDS, 10% mercaptoetanol, 0.125 M Tris-HCl, 20% glycerol, 0.004% bromophenol blue) and boiled for 5 min at 95ºC. After removal of the magnetic beads, samples were resolved by SDS-PAGE and probed for proteins of interest through western blotting. For Western blot analysis, resolved proteins were transferred to a nitrocellulose membrane, using the iBlot Dry Blotting System (Invitrogen) according to the manufacturer's instructions. Transferred proteins were confirmed by ponceau staining (0.25% Ponceau S in 40% methanol and 15% acetic acid). The membrane was blocked for 3 hour at room temperature with 5% dry milk in PBST. All the primary and secondary antibodies were diluted in PBST containing 1% BSA and the membranes were incubated overnight at 4ºC under agitation, then washed three times 10 min with PBST and immediately incubated with secondary antibodies diluted in 1% dry milk in PBST 1 hour at room temperature under agitation. Anti-rabbit, anti-mouse and anti-guinea pig secondary antibodies conjugated to Horseradish peroxidase (Amersham) were

used according to the manufacturer's instructions. Blots were developed with ECL Chemiluminescent Detection System (Amersham) according to manufacturer's protocol and detected on X-ray film (Fuji Medical X-Ray Film). To confirm protein hyperphosphorylation status, 50 µg of control cell lysates were treated with 20 U of alkaline phosphatase (Fermentas, FastAP) for 1 hour at 37ºC. A GS800 densitometer and Quantity One software (Bio-Rad) were used for quantitative immunoblotting when required.

2.10. Kinase assays

For *in vitro* phosphorylation assays, His6-DmMps1^{KD}, His6-DmMps1$^{150-379}$ or Casein were incubated with active Polo (a gift from Bill Sullivan), His6-DmMps1^{WT} or HsMps1 (SignalChem) for 30 minutes in a total volume of 30 µL of kinase reaction buffer (5 mM MOPS pH 7.4, 2.5 mM β-glycerol-phosphate, 5 mM $MgCl_2$, 1 mM EGTA, 0.4 mM EDTA, 0.25 mM DTT, 100 µM ATP and 10 µCi [γ-^{32}P]ATP [3000 Ci/mmol, 10 mCi/mL]). Kinase reactions were carried out at 25ºC for Polo or His6-DmMps1^{WT} and at 30ºC when using HsMps1. For inhibition of HsMps1, 10 µM MPS1-IN-1 (a gift from Helder Maiato) were added in a final volume of 1 mL DMSO. Reactions were stopped by addition of Laemmli sample buffer (4% SDS, 10% mercaptoetanol, 0.125 M Tris-HCl, 20% glycerol, 0.004% bromophenol blue) and heated for 5 min at 95ºC. The labeled proteins were resolved in an 8% SDS-PAGE, stained with Coomassie Blue and radioactive phosphate incorporation was detected on X-Ray film (Fuji Medical X-Ray Film).

2.11. Antibodies

The primary antibodies used were anti-α-tubulin mouse B512 (Sigma) at 1:4000 for immunofluorescence (IF), anti-α-tubulin mouse DM1A (Sigma) at 1:10000 for immunoblotting (IB), anti-phosphorylated ser10-Histone H3 rabbit (Upstate Biotechnology) at 1:10000 (IF), anti-CID rat (Martins et al., 2009) at 1:500 (IF), anti-Mps1 guinea pig (Gp15) (gift from Scott Hawley) at 1:500 (IF), 1:5000 (IB), 1:50 for immunoprecipitation (IP), anti-Mps1^{T490Ph} rabbit (gift from Geert Kops) at 1:10000 (IF), anti-Polo mouse at 1:50

(IB), 1:50 (IP), anti-Polo^{T210Ph} (ab39068) mouse (Abcam) at 1:5000 (IF), anti-Megator mouse (gift from Helder Maiato) at 1:40 (IF), anti-EGFP rabbit (gift from Frederico Silva) at 1:100 for immunoprecipitation (IP) and 1:1000 (IF), anti-RFP rabbit (Invitrogen) at 1:100 (IP), anti-GFP rabbit (Molecular Probes) at 1:100 (IP). Secondary antibodies conjugated with horseradish peroxidase (HRP, Santa Cruz Biotechnology) for immunoblotting were used according to the manufacturer's instructions, anti-mouse HRP at 1:5000, anti-guinea pig HRP at 1:2000 and anti-rabbit HRP at 1:15000.

For immunofluorescence the secondary antibodies fluorescence dyes from Alexa Fluor® (Invitrogen) were used at 1:2000 with the exception of Alexa Fluor® 647 conjugated ones, which were used at 1:1000.

2.12. FRAP analysis

The FRAP experiments were performed in S2 cells expressing EGFP-Mps1^{WT}, EGFP-Mps1^{KD}, EGFP-Mps1^{4D} and EGFP-Mps1^{4A} treated with MG132 for 1 h followed by a 2 h treatment with colchicine. When required, 100 nM BI2536 were added 60 min prior FRAP measurement. Data sets were collected at 25ºC with a Leica TCS SP5II scanning confocal microscope (Leica Microsystems, Germany). The EGFP tag of Mps1 was excited using the 488 nm laser line set to 10% and bleached with the 405 nm laser line. Single kinetochores were bleached for four iterations once the fluorescence signal of EGFP-Mps1 had become stable. Fluorescence intensity in the bleached area was acquired every 555 ms before and after bleaching. FRAP data analysis was performed with ImageJ. For each measurement, the average fluorescence intensity in the bleached area was corrected for background and the ratio to average fluorescence in the cytoplasm determined. Average values before bleaching were set to 100%. The exponential kinetics of FRAP were analysed by calculating the normalized unrecovered fluorescence at each time point (Finf_F(t))/(Finf_F(0)) where Finf is the value reached at the plateau, F(0) is the value observed in the first frame after bleaching and F(t) is the value at a given time point. FRAP kinetics parameters were determined by one-exponential curve fitting to normalized data using GraphPad Prism software.

2.13. Time-lapse microscopy

Live analysis of mitosis was done in S2 cell lines expressing the indicated constructs. After the desired treatment, cells were plated in MarTek glass bottom dishes (MatTek Corporation) previously treated with Concanavalin A (Sigma) at 25 mg mL^{-1}. 4D data sets were collected at 25ºC with a spinning disc confocal system (Revolution; Andor) equipped with an electron multiplying charge-coupled device camera (iXonEM+, Andor) and a CSU-22 unit (Yokogawa) based on an inverted microscope (IX81; Olympus). Two laser lines (488 and 561 nm) were used for near-simultaneous excitation of EGFP and mCherry/mRFP. The system was driven by iQ software (Andor). Time-lapse imaging of z stacks with 0.8 µm steps covering the entire volume of the cell were collected every 30, 60, 120 or 300 seconds. Image sequence analysis and video assembly were done with ImageJ.

CHAPTER 3

RESULTS

3.1. Polo regulates Mps1 kinetochore localization and activation

Kinetochore localization of Mps1 is suggested to control its kinase activity and to be required for sustained SAC activity (Jelluma et al., 2008; Stucke et al., 2002). Upon mitotic entry, Aurora B acts in concert with the Ndc80 complex to promote Mps1 kinetochore recruitment and activation (Santaguida et al., 2011; Saurin et al., 2011). The N-terminal non-catalytic domain was shown to be necessary and sufficient for this process in human cells (Maciejowski et al., 2010; Stucke et al., 2004). Nevertheless, it has been suggested that the C-terminal domain of Mps1 also regulates kinetochore targeting, possibly by masking its N-terminal, pending adequate stimulus (Xu et al., 2009; Zhao and Chen, 2006). Interestingly, in *Drosophila*, Mps1 kinetochore recruitment is mediated by the catalytic C-terminal with the N-terminal being dispensable for the process. Moreover, Mps1 kinase activity is required for kinetochore localization in flies (Althoff et al., 2012), in contrast to recent observations in mammalian cells (Hewitt et al., 2010; Jelluma et al., 2010).

Kinetochore localization of Mps1 is suggested to increase its local concentration, which favors its dimerization and subsequent activation by *trans* autophosphorylation (Hewitt et al., 2010; Kang et al., 2007). Among the several identified autophosphorylation residues, conserved Thr^{676} in the T-loop was shown to be essential for Mps1 full kinase activity and may potentiate further activating phosphorylation in residue Thr^{686} which was proposed to be critical for proper orientation of a conserved Lys residue important for anchoring substrate and ATP in the catalytic loop (Kang et al., 2007; Mattison et al., 2007; Wang et al., 2009). Notwithstanding Mps1 prominence in SAC signaling, the precise molecular events controlling its kinetochore localization and activation still need to be uncovered.

Comparison of Mps1 activation loops from several organisms shows that Thr^{676} is conserved in several metazoan Mps1 proteins including *Drosophila* (Figure 3.1.1A). To monitor Mps1 activity at kinetochores in flies, we used a phosphospecific antibody against phosphorylated Thr^{490} in the activation loop of *Drosophila* Mps1 (equivalent to human Thr^{676}). Phosphorylation of this site has been used previously as a marker for Mps1 activation (Saurin et al., 2011). Immunofluorescence analysis in S2 cells (Figure 3.1.1B) revealed that Mps1 T-loop activation becomes detectable during prophase in the nucleoplasm and pre-kinetochores. As expected, Mps1 activation is prominently elevated at unattached prometaphase kinetochores. As chromosomes congress to the metaphase

plate, Mps1^{T490Ph} signal severely decreases becoming undetectable during anaphase and interphase. This Mps1 activation pattern is consistent with the reported for human Mps1 orthologue (Saurin et al., 2011). As in mammalian cells, the centrosomic staining observed with this antibody is nonspecific as does not change upon Mps1 depletion (data not shown).

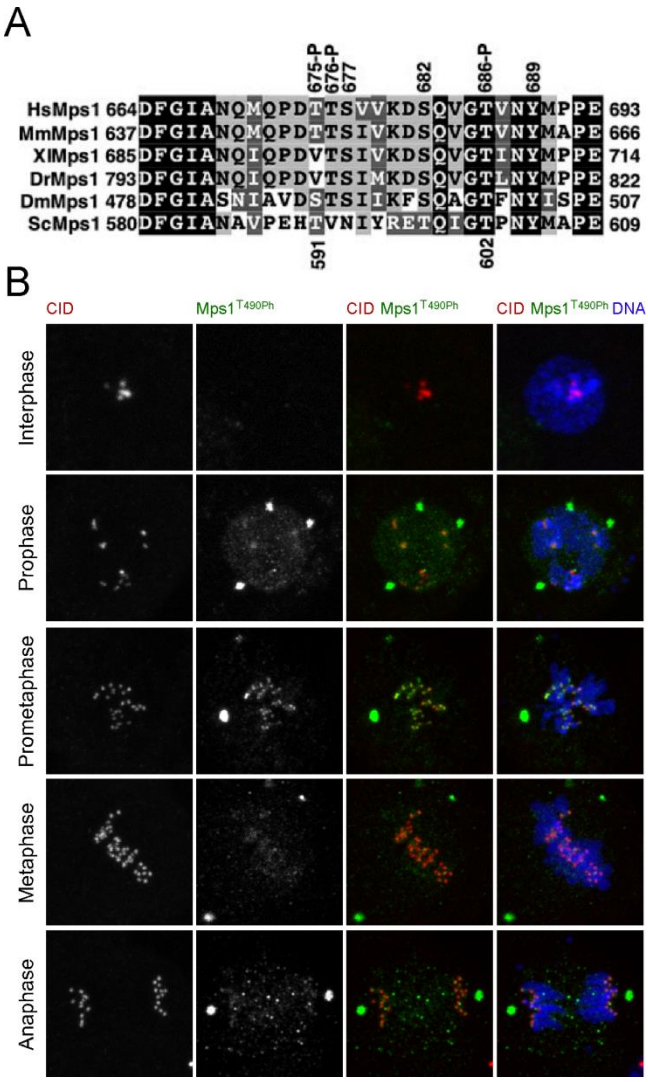

Figure 3.1.1 - Localization pattern of Mps1-T-loop phosphorylation through mitosis. (A) Conservation among Mps1 activation loop residues. The alignment indicates conservation among Mps1 proteins at positions Thr686 and Tyr689, whereas Ser682 is similar. Residues Thr676 and Ser677 are conserved within metazoan Mps1 proteins. The numbers note specific residues for hMps1 and yeast Mps1, and P indicates a phosphorylated residue. Identical residues are indicated by a black background with white lettering, conserved residues are indicated by gray background with black lettering, and similar residues are indicated by gray background with white lettering (from Mattison et al., 2007). (B) Immunofluorescence analysis of asynchronous S2 cells stained for Mps1^{T490} phosphorylation (Mps1^{T490Ph}). CID was stained as a kinetochore reference.

Conde and colleagues have recently implicated Polo as a factor involved in the kinetochore localization of Mps1 (Conde et al., 2013a). In agreement with previous data, RNAi-mediated depletion of Polo in S2 cells caused a 40-50% reduction in the recruitment of Mps1 to unattached kinetochores (Figure 3.1.2A, B). To examine if this reduction affected Mps1 activation, we assayed by immunofluorescence the kinetochore levels of $Mps1^{T490Ph}$. As expected, Polo depletion led to a dramatic decrease in kinetochore-localized Mps1 activity (Figure 3.1.2A, B). Surprisingly, inhibition of Polo activity with the specific inhibitor BI2536 promoted a notorious increase of Mps1 kinetochore levels (150%) that was not paralleled by an increment in Mps1 activity (Figure 3.1.2A, B). Polo inhibition impaired proper Mps1 activation at kinetochores similarly to the observed in Polo-depleted cells indicating that Polo activity is required for Mps1 activation at kinetochores even when its recruitment is not negatively affected.

Studies *in vivo* and *in vitro* have shown that Mps1 dimerization induces its trans-autophosphorylation and consequently its activation (Kang et al., 2007). To determine whether Mps1 is able to dimerize upon Polo inhibition, we expressed EGFP-Mps1 in cells treated with BI2536, followed by analysis of co-immunoprecipitation. Endogenous Mps1 was found to co-immunoprecipitate with EGFP-Mps1 immunoprecipitates in a yield similar to the obtained for control untreated cells, suggesting that Polo activity is not required for Mps1 self-interaction (Figure 3.1.2C). Taken together, these results show that kinetochore accumulation of endogenous Mps1 and its dimerization are not sufficient to drive its activation and those other factors such as Polo activity, are required for the process.

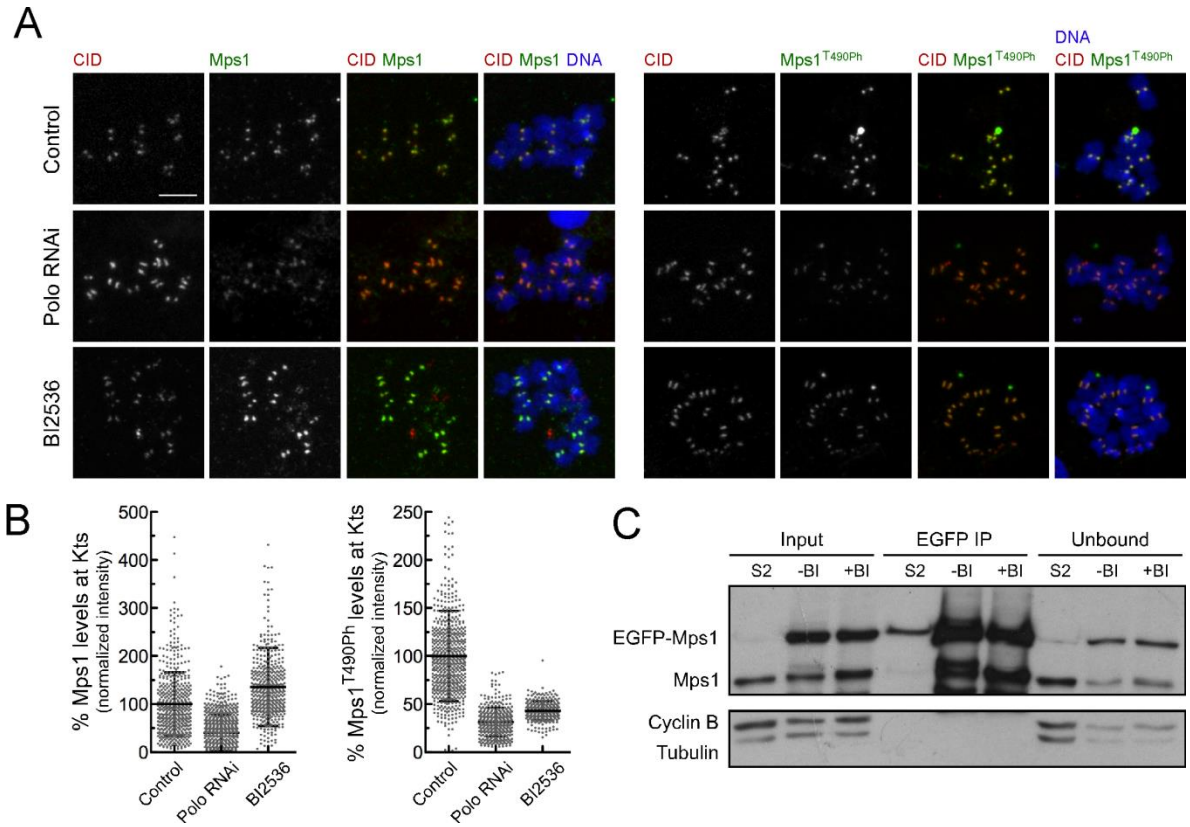

Figure 3.1.2 - Polo regulates Mps1 kinetochore localization and activation. (A) Immunofluorescence analysis of Mps1 localization and Mps1^{T490} phosphorylation (Mps1^{T490Ph}) at kinetochores. (B) Quantification of experiment in (A). Mps1 and Mps1^{T490Ph} fluorescence intensities were determined relative to CID. Data represent means ± s.d. and mean values obtained for control cells were set to 100%. (C) Immunoprecipitation of EGFP-Mps1 from total cells lysates obtained from untransfected S2 cells, S2 cells expressing EGFP-Mps1 (-BI) and S2 cells expressing EGFP-Mps1 treated with BI2536 (+BI). Immunoprecipitates (IP) and corresponding total cell lysates (Input) and unbound fractions were probed by immunoblotting for the indicated proteins. For (A) and (C) Cultured cells were treated with MG132 for 1 hour followed by a 2 hours period of colchicine incubation. For Polo inhibition, BI2536 was added to cultures simultaneously with colchicine. Scale bar represent 5 µm.

3.2. Polo promotes Mps1 activation and nuclear import during prophase

Mps1 kinase activity was shown to be required for its kinetochore recruitment in *Drosophila* (Althoff et al., 2012). However, inhibition of Polo with BI2536 caused an overaccumulation of inactive Mps1 at kinetochores. To reconcile these findings one must consider the timing at which cells lost Polo activity. Polo-depleted mitotic cells entered mitosis in the absence of Polo activity, whereas in cultured cells treated with BI2536,

inhibition of Polo occurred mandatorily after mitotic entry (BI2536 and MG132 preclude mitotic entry during the time-frame of the experience; please report to the legend of Figure 3.1.2). We hypothesize that during prophase, Polo activity contributes to the initial activation of Mps1 required to drive the bulk of its kinetochore recruitment upon nuclear envelope breakdown (NEB). Polo activity is continuously required during prometaphase to maintain Mps1 active at kinetochores. However, impairing the activation of kinetochore-associated Mps1 does not result in its dissociation from these structures.

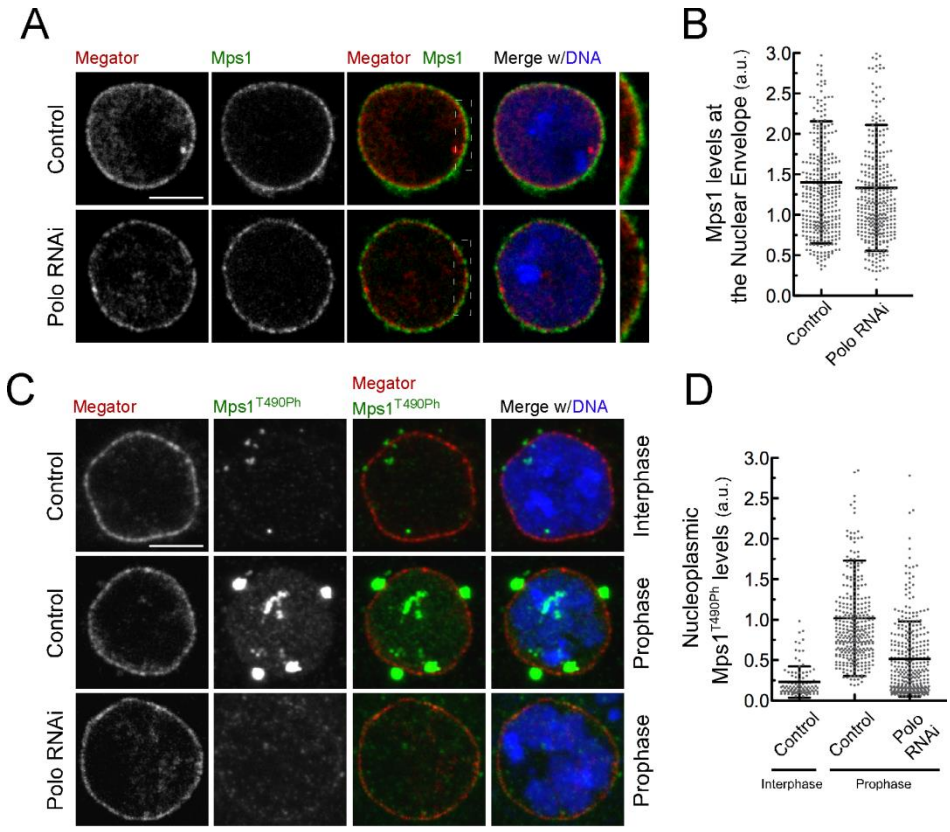

Figure 3.2.1 - Polo promotes Mps1 activation and nuclear import during prophase. Immunolocalization of Mps1 (A) and Mps1^{T490Ph} (C) at the nuclear envelope and nucleoplasm. (B) Quantification of experiment in (A). (D) Quantification of experiment in (C). Mps1 and Mps1^{T490Ph} fluorescence intensities were determined relative to Megator fluorescence intensity. Data represent mean ± s.d. Scale bars represent 5 µm.

Mps1 localizes to the nuclear envelope of S2 cells throughout interphase and prophase as assessed by immunofluorescence analysis (Figure 3.2.1A). 3D-structured illumination microscopy (3D-SIM) further revealed that Mps1 localizes to the cytoplasmic side of nuclear pores (Carlos Conde and Paula Sampaio, unpublished data). Live-cell imaging of S2 cells expressing Polo-EGFP allowed us to observe an enrichment of Polo at the nuclear envelope immediately before NEB (Figure 3.2.2A, B). Moreover, a

phosphospecific antibody that was previously shown to recognize *Drosophila* Polo-T-loop activating phosphorylation by Aurora kinases (Polo^{T182Ph}) (Carmena et al., 2012; Conde et al., 2013a) revealed that Polo becomes active at the nuclear pore during prophase (Figure 3.2.2C).

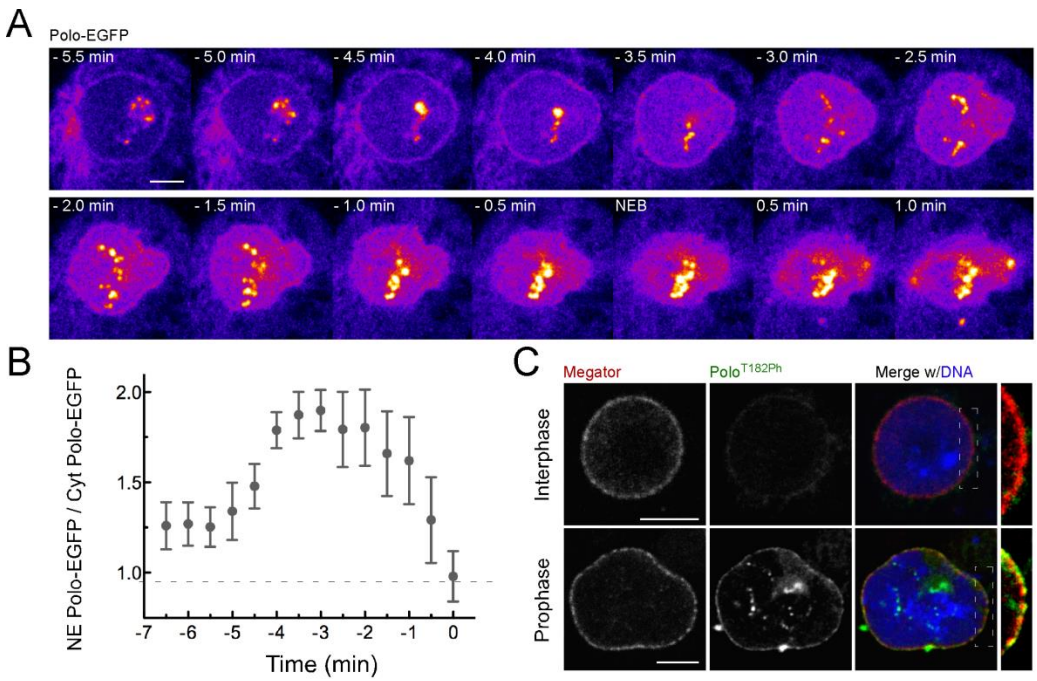

Figure 3.2.2 - Active Polo localizes at the nuclear envelope during prophase. (A) Mitotic progression of S2 cells expressing Polo-EGFP was monitored by time-lapse microscopy. Selected stills are present and respective time is shown in min. (B) Quantification of Polo-EGFP fluorescence intensity at nuclear envelope relative to the cytoplasmic signal plotted against time. (C) Immunofluorescence analysis of Polo^{T182} phosphorylation (PoloT^{182Ph}) during interphase and prophase. Megator staining was used as nuclear envelop reference. The insets show higher-magnification views of boxed areas. Data represent mean ± s.d. Scale bars represent 5 µm.

It is therefore tempting to speculate that active Polo promotes the initial activation of Mps1 at the nuclear envelope or at nuclear pores immediately before mitotic entry. In line with this, we found that Polo depletion resulted in a significant reduction of nucleoplasmic Mps1^{T490Ph} in prophase (Figure 3.2.1C, D) without affecting Mps1 localization at the nuclear envelope (Figure 3.2.1A, B). Intriguingly, we failed to detect Mps1^{T490Ph} staining at the nuclear envelope of control S2 cells during prophase, which might indicate that Mps1 is imported into the nucleus once activated. To examine whether the nuclear import of active Mps1 is promoted by its activation or regulated by Polo activity at the nuclear envelope, we overexpressed EGFP-Mps1^{WT} in interphase cells to drive its auto-activation when Polo activity is kept at basal levels. Under these circumstances,

active Mps1 is promptly found in the cytoplasm and at the nuclear envelope but fails to be detected in the nucleus (Figure 3.2.3A-C), suggesting that Polo activity is required to promote the nuclear import of active Mps1. To test this, we generated S2 cell lines expressing either wild-type Polo (Polo^{WT}-EGFP) or constitutively active Polo carrying the phosphomimetic T182D mutation (Polo^{T182D}-EGFP). Expression of Polo^{T182D}-EGFP, but not Polo^{WT}-EGFP, was able to promote the activation of endogenous Mps1 in interphase cells, with Mps1-T-loop phosphorylation being detected in the cytoplasm and nucleoplasm but not at the nuclear envelope (Figure 3.2.3D, E). Cumulatively, these results suggest that in addition to its contribution for Mps1 activation, Polo has a role in promoting the nuclear import of Mps1 in its active form.

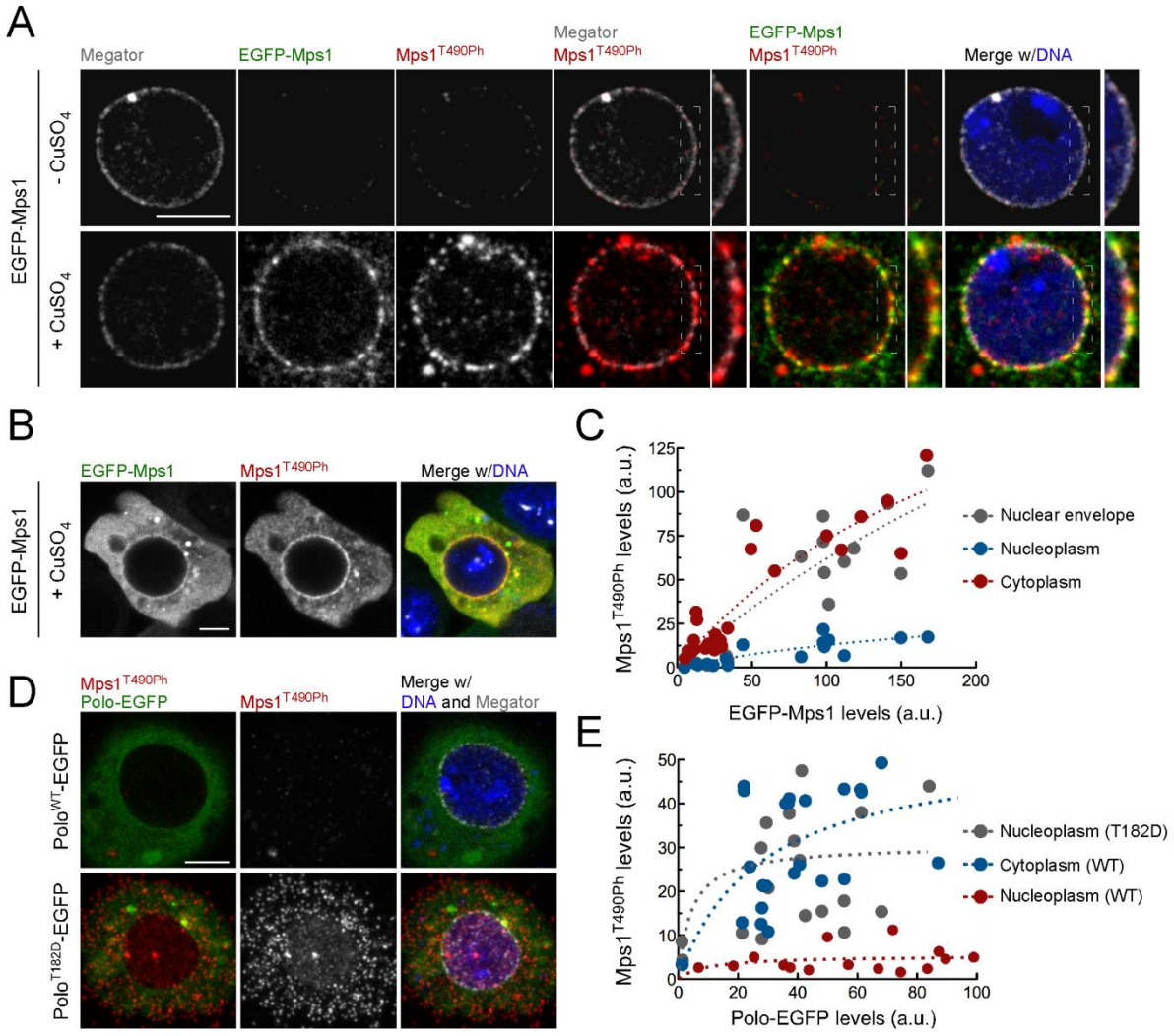

Figure 3.2.3 - Polo promotes the nuclear import of active Mps1 during prophase. (A) Immunofluorescence analysis of EGFP-Mps1 and Mps1^{T490Ph} at the nuclear envelope of interphase cells overexpressing EGFP-Mps1. (B) Immunofluorescence analysis of EGFP-Mps1 and Mps1^{T490Ph} at the cytosol and nuclear pore of interphase cells

overexpressing EGFP-Mps1. The insets show higher-magnification views of boxed areas. (C) Quantification of $Mps1^{T490Ph}$ levels plotted against EGFP-Mps1 levels from experiment in (B). (D) Immunolocalization of Polo-EGFP and $Mps1^{T490Ph}$ in interphase cells expressing $Polo^{WT}$-EGFP and $Polo^{T182D}$-EGFP. (E) Quantification of $Mps1^{T490Ph}$ levels plotted against Polo-EGFP levels from experiment in (D). Scale bars represent 5 µm.

3.3. Polo controls Mps1 dissociation from kinetochores

Previous work has shown that Polo regulates Mps1 kinetochore recruitment indirectly by controlling the levels of Ndc80 at kinetochores (Conde et al., 2013a). In the present work we found that Polo further contributes to Mps1 kinetochore localization by promoting its initial activation at the nuclear envelope/pore during prophase deemed necessary for the process in *Drosophila*. Addition of BI2536 to cultured S2 cells impaired Mps1 activation at kinetochores but intriguingly resulted in a 50% increase of the protein at this site. This indicates that Polo activity is continuously required to maintain Mps1 activation at kinetochores during prometaphase and that, if Polo inhibition occurs after mitotic entry, the levels of Mps1 at these sites increase. To confirm this, we monitored by live-cell imaging EGFP-Mps1 levels at kinetochores after Polo inhibition. Addition of BI2536 to prometaphase cells caused a 4-fold increase of exogenous EGFP-Mps1 levels at kinetochores relative to control cells treated with DMSO (Figure 3.3.1A, B).

Previous work in the lab has shown that depletion of Polo in *Drosophila* results in the formation of highly stable syntelic attachments (Moutinho-Santos et al., 2012). In agreement with that and contrasting with the reported for human cell lines, we found that S2 cells treated with BI2536 also display a high percentage of kinetochore pairs attached to the mitotic spindle in a syntelic orientation (Figure 3.3.1C, E). Interestingly, this kinetochores stably bound to spindle microtubules were able to retain high levels of inactive Mps1 when compared to kinetochores mediating amphitelic attachments in control cells (Figure 3.3.1C-E).

To examine whether Polo inhibition affected Mps1 dynamic exchange at unattached kinetochores, we performed FRAP analysis in S2 cells expressing EGFP-$Mps1^{WT}$ treated with colchicine. Similarly to the observed in human cells (Jelluma et al., 2010), *Drosophila* Mps1 is highly dynamic at kinetochores showing a monophasic recovery after photobleaching of ~ 80% with a half-time of ~ 1 s (Figure 3.3.1F). Addition of BI2356 caused Mps1 half-life to increase 6-fold and recovery was reduced to 75% (Figure 3.3.1F). This result indicates that Polo activity is required for Mps1 dynamic exchange at

kinetochores, which may underlie the higher protein levels detected by immunofluorescence and by live-cell imaging after BI2535 addition (Figure 3.1.2A, B and Figure 3.3.1A, B).

Human Plk1 was shown to promote kinetochore localization of PP2A-B56α phosphatase through phosphorylation of BubR1 KARD domain (Suijkerbuijk et al., 2012). This domain is conserved in flies and to examine whether the observed reduction in Mps1 kinetochore dynamics upon Polo inhibition results from an impairment of PP2A-B56α recruitment we performed FRAP analysis of EGFP-Mps1 in S2 cells depleted of BubR1. Loss of PP2A-B56α from kinetochores had no noticeable effect on Mps1 kinetics at kinetochores (Figure 3.3.1F). A similar result was obtained upon depletion of PP1-87B phosphatase (Carlos Conde, unpublished) indicating that the mechanism by which Polo controls Mps1 exchange rate at kinetochores does not involve the action of *Drosophila* main phosphatases.

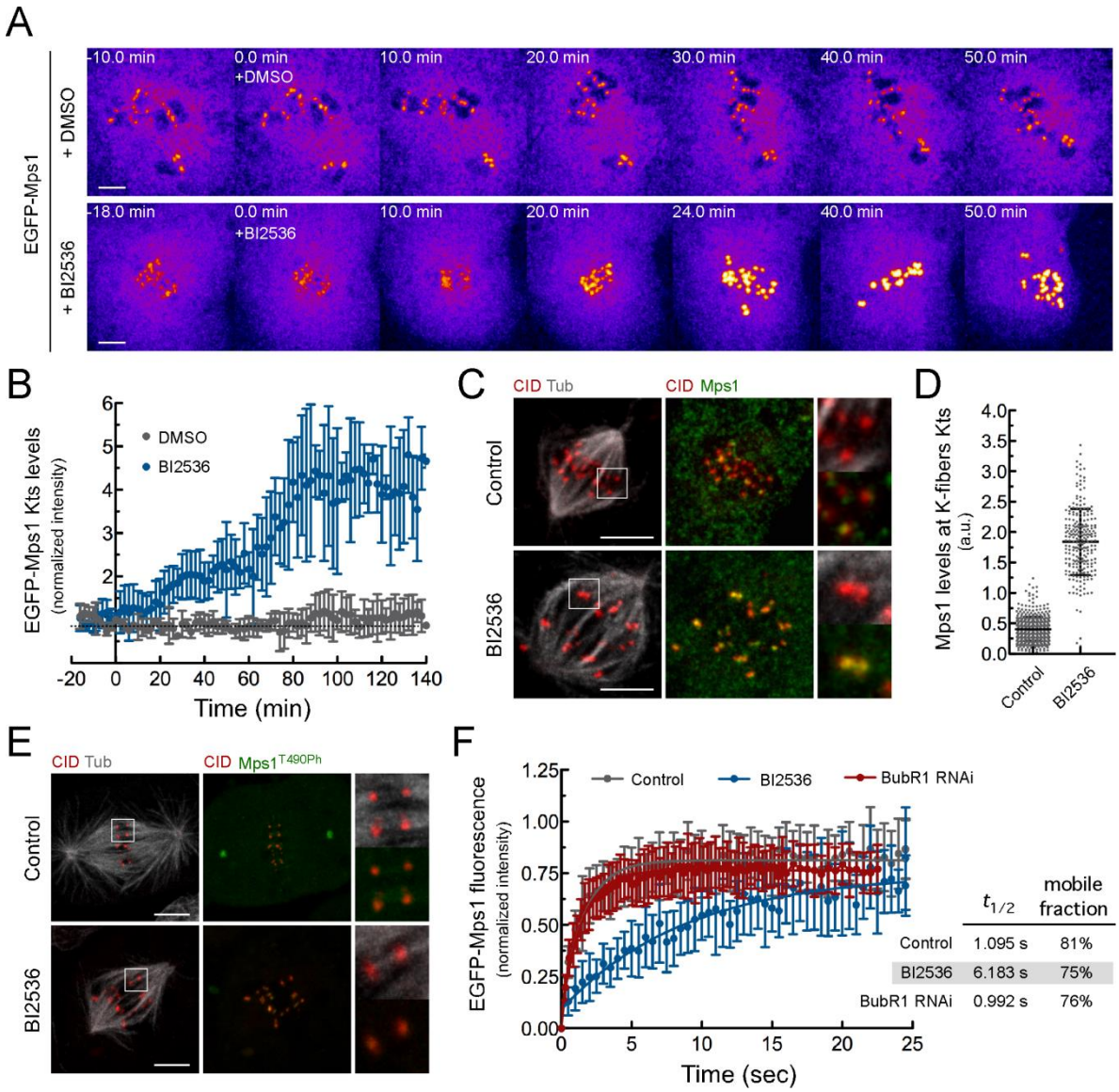

Figure 3.3.1 - Polo controls Mps1 dissociation from kinetochores. (A) Mitotic progression of DMSO or BI2536-treated cells expressing EGFP-Mps1 was monitored by time-lapse microscopy. Selected stills of live-imaging are depicted and respective time shown in min. (B) Quantification of Mps1 signal intensity at kinetochores was corrected for cytosolic signal intensity and plotted against time. Immunofluorescence analysis of Mps1 (C) and Mps1^{T490Ph} (E) levels at kinetochores attached to K-fibers. The insets show higher-magnification views of boxed areas. (D) Quantification of experiment in (C). Mps1 fluorescence intensities were determined relative to CID. Data represent means ± s.d. (F) FRAP analysis of EGFP-Mps1 for each of the indicated conditions after bleaching of single kinetochores. Graph shows average fluorescence intensities ± s.e. n= 20 cells/condition. Recovery half-life and mobile fraction are depicted. For (A), (C) and (D) BI2536 was added to asynchronous cultured cells. For (F), cultured cells were treated with MG132 for 1 hour followed by a 2 hours period of colchicine incubation. When required, BI2536 was added to cultures simultaneously with colchicine. Scale bar represent 5 µm.

In human cells, Mps1 activity was shown to contribute for its dynamic behavior (Jelluma et al., 2010). However, FRAP analysis of a kinase dead version of Mps1 (EGFP-Mps1^{KD}) revealed a similar half-life of recovery to EGFP-Mps1^{WT} and a modest increase (10%) of the non-exchanging pool of kinetochore-bound Mps1 (Figure 3.5.2C), suggesting that the observed increment in Mps1 kinetochore residence time unlikely results from impaired Mps1 activity caused by Polo inhibition. One must however consider a possible contribution of endogenous Mps1 in promoting EGFP-Mps1^{KD} dynamic exchange at kinetochores. Nevertheless, pharmacological inhibition of Mps1 in human cells caused no more than a 1.5 fold increase in Mps1 half-life at kinetochores, indicating that the exchange of Mps1, although influenced by it, is not fully dependent on its kinase activity (Jelluma et al., 2010). Taken together, these results indicate the Polo activity is required to promote Mps1 rapid release from kinetochores.

3.4. Polo phosphorylates Mps1 N-terminal

Results presented above indicate that Polo is required for Mps1 activation in early mitosis and through prometaphase and seems to exert a dual regulation over Mps1 kinetochore localization.

To examine whether Polo and Mps1 can interact *in vivo* we performed reciprocal co-immunoprecipitation experiments using lysates of cells treated with colchicine and MG132. As shown by immunoblotting, Mps1 could be readily detected in Polo immunoprecipitates, and, similarly, Polo was present in Mps1 immunoprecipitates (Figure 3.4.1A) indicating that the two kinases are found in a complex *in vivo*. To test if Polo directly phosphorylates Mps1 we performed *in vitro* kinase assays using recombinant proteins expressed in baculovirus-infected Sf21 insect cells. As expected, recombinant His6-DmMps1^{WT} displayed auto-phosphorylation activity, which precludes accurate assessment of any Polo-catalyzed phosphorylation (Figure 3.4.1B). To circumvent this, we produced a recombinant kinase-dead version of Mps1 (His6-DmMps1^{KD}) to test as a Polo substrate. In accordance with an impairment of its kinase activity, we failed to detect Mps1^{KD} autophosphorylation or casein phosphorylation (Figure 3.4.1B). We also failed to find any significant increment of ^{32}P incorporation in His6-DmMps1^{KD} when active Polo was added to the reaction, thus indicating that under these *in vitro* conditions, Polo is unable to phosphorylate full-length Mps1 (Figure 3.4.1B, C). However, Polo was able to

phosphorylate a bacterially expressed N-terminal region of Mps1 (His6-DmMps1$^{150-379}$) under the same reaction conditions (Figure 3.4.1C). Since the baculovirus-Sf21 system allows proteins to be expressed in their native conformation, we speculate that His6-DmMps1^{KD} is folded in way that conceals its N-terminal region, thus hindering its phosphorylation by Polo.

To test if Mps1 autophosphorylation induces a conformational change that renders the previously cryptic N-terminal now accessible to Polo, we used active human Mps1 (HsMps1) and its specific inhibitor Mps1-IN-1 (Kwiatkowski et al., 2010). HsMps1 has the capacity to directly phosphorylate His6-DmMps1^{KD} and the addition of Mps1-IN-1 to the reaction causes a potent inhibition of HsMps1 as judged by the severe decrease in its autophosphorylation and in the phosphorylation of His6-DmMps1^{KD} (Figure 3.4.1D). To test if autophosphorylation of Mps1 is required to allow its phosphorylation by Polo we performed a first reaction with active human Mps1 (HsMps1) and His6-DmMps1^{KD} in the presence of unlabeled ATP. The reaction was stopped by the addition of Mps1-IN-1 and followed by a second reaction to which Polo and radioactive ATP were added. Under these conditions, we were able to detect phosphorylation of His6-DmMps1^{KD}, supporting the notion that Mps1 autophosphorylation likely induces a structural rearrangement exposing the protein N-terminal region, which, consequently becomes phosphorylated by Polo (Figure 3.4.1D). In line with this, *in silico* analysis predicts the existence of 4 putative Polo phosphorylation sites (Thr^{185}, Thr^{197}, Thr^{260}, Ser^{262}) within the Mps1 N-terminal region spanning from amino acids 150 to 379 (Figure 3.4.1E, F). Importantly, the inability of Polo to phosphorylate catalytic inactive Mps1 suggests that the mechanism by which Polo contributes for its initial activation during prophase is either indirect or requires additional factors.

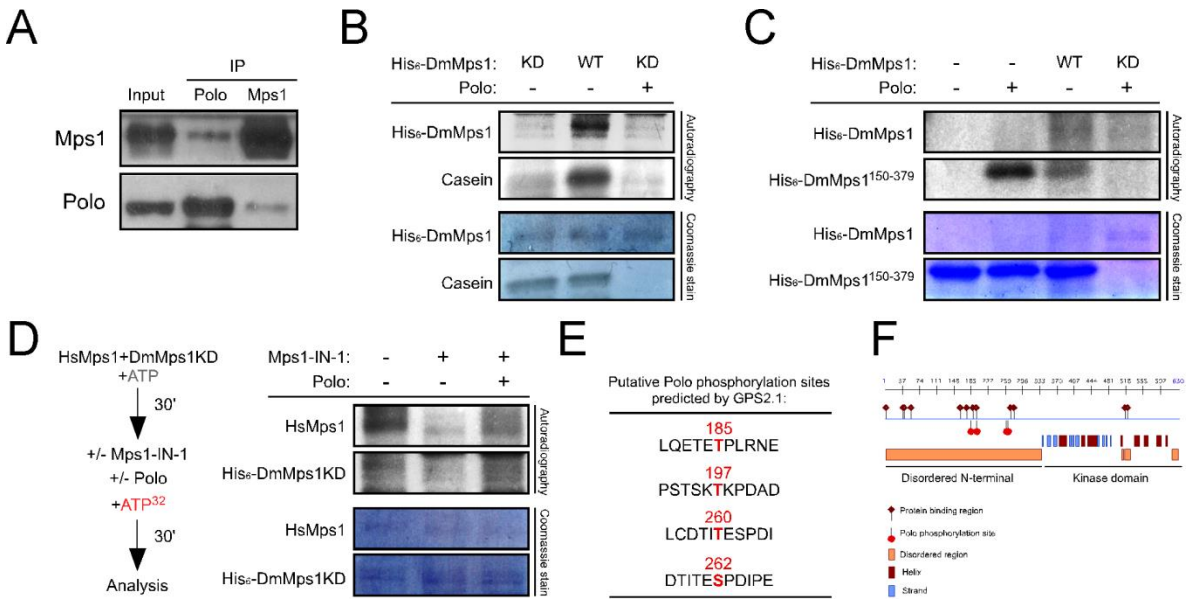

Figure 3.4.1 - Polo interacts with Mps1 *in vivo* and phosphorylates Mps1 N-terminal *in vitro*. (A) Immunoprecipitation of Polo and Mps1 from total cell lysates obtained from S2 cells treated with colchicine. Immunoprecipitates (IP) and corresponding total cell lysates (Input) were probed by immunoblotting for the indicated proteins. (B) Kinase assay with recombinant *Drosophila* $Mps1^{WT}$ and $Mps1^{KD}$. Casein was used as substrate to assess the activity of both versions of Mps1 kinase. (C) Kinase assay with active Polo and recombinant $Mps1^{KD}$ and $Mps1^{150-379}$ fragment as substrates. (D) Two-step kinase assay using HsMps1/TTK and cold ATP followed by the addition of Polo, ATP^{32} and HsMps1/TTK specific inhibitor Mps1-IN-1. $DmMps1^{KD}$ was used as substrate. (E) *In silico* analysis (GPS2.1.) of $Mps1^{150-379}$ for Polo phosphorylation sites. (F) Schematic representation of Mps1 domain organization predicted *in silico* (ProteinPredict). Putative Polo phosphorylation sites are depicted.

3.5. Polo phosphorylation of Mps1 N-terminal restrains Mps1 activity and regulates its dissociation from kinetochores

To analyze the functional relevance of Mps1 phosphorylation by Polo, we generated S2 cell lines expressing nonphosphorylatable $Mps1^{T185A,\ T197A,\ T260A,\ S262A}$ (EGFP-$Mps1^{4A}$) and the corresponding phosphomimetic $Mps1^{T185D,\ T197D,\ T260D,\ S262D}$ (EGFP-$Mps1^{4D}$). Immunofluorescence analysis upon colchicine treatment revealed that EGFP-$Mps1^{4A}$ and EGFP-$Mps1^{4D}$ are able to localize to unattached kinetochores (Figure 3.5.1A). However, comparing to EGFP-$Mps1^{WT}$, mimicking Polo phosphorylation leads to a slight decrease of EGFP-Mps1 kinetochore levels (to 74%) whereas impairing phosphorylation of the predicted Polo sites results in a modest but significant increase of EGFP-Mps1 recruitment to unattached kinetochores (to 115%) (Figure 3.5.1C). To examine the consequence of these mutations on Mps1 activation, we determined the kinetics of Mps1-

T-loop phosphorylation in cells expressing the transgenes. Variation of kinetochore-associated Mps1^{T490Ph} with the levels of EGFP-Mps1 at kinetochores shows that T-loop phosphorylation of the analyzed mutants occurs to a similar extent as in EGFP-Mps1^{WT} (Figure 3.5.1A, D). However, no conclusion can be drawn from the effect of these mutations on the kinase activity since endogenous active Mps1 is likely contributing for T-loop phosphorylation of exogenous Mps1. This would explain why the levels of kinetochore Mps1^{T490Ph} in cells expressing catalytic inactive Mps1 (EGFP-Mps1^{KD}) are similar to the quantified in cells expressing EGFP-Mps1^{WT} (Figure 3.5.1A, D). Due to technical limitations we were not able to efficiently deplete endogenous Mps1 in cells expressing EGFP-Mps1 transgenes.

Given that the presence of endogenous Mps1 precludes us from evaluating the effect of the mutations on Mps1 activity during mitosis, we quantified the levels of cytosolic Mps1^{T490Ph} in interphase cells, when endogenous Mps1 is known to be inactive. Similar to what we observed in S2 cells without transgenes (Figure 3.1.1B) but contrasting with expression of EGFP-Mps1^{WT}, we failed to detect Mps1^{T490Ph} staining in interphase cells upon expression of EGFP-Mps1^{KD} hence validating the experimental setup (Figure 3.5.1B, E). Interestingly, expression of EGFP-Mps1^{4D} consistently resulted in lower levels of cytosolic Mps1^{T490Ph} when compared with EGFP-Mps1^{WT} expressed at identical levels (Figure 3.5.1B, E), suggesting that Polo-mediated phosphorylation of Mps1 N-terminal has an inhibitory effect on Mps1 activity. Conversely, EGFP-Mps1^{4A} became promptly activated even when expressed at lower levels than EGFP-Mps1^{WT} (Figure 3.5.1B, E) further suggesting an inhibitory role of Mps1 N-terminal that is potentiated by Polo phosphorylation.

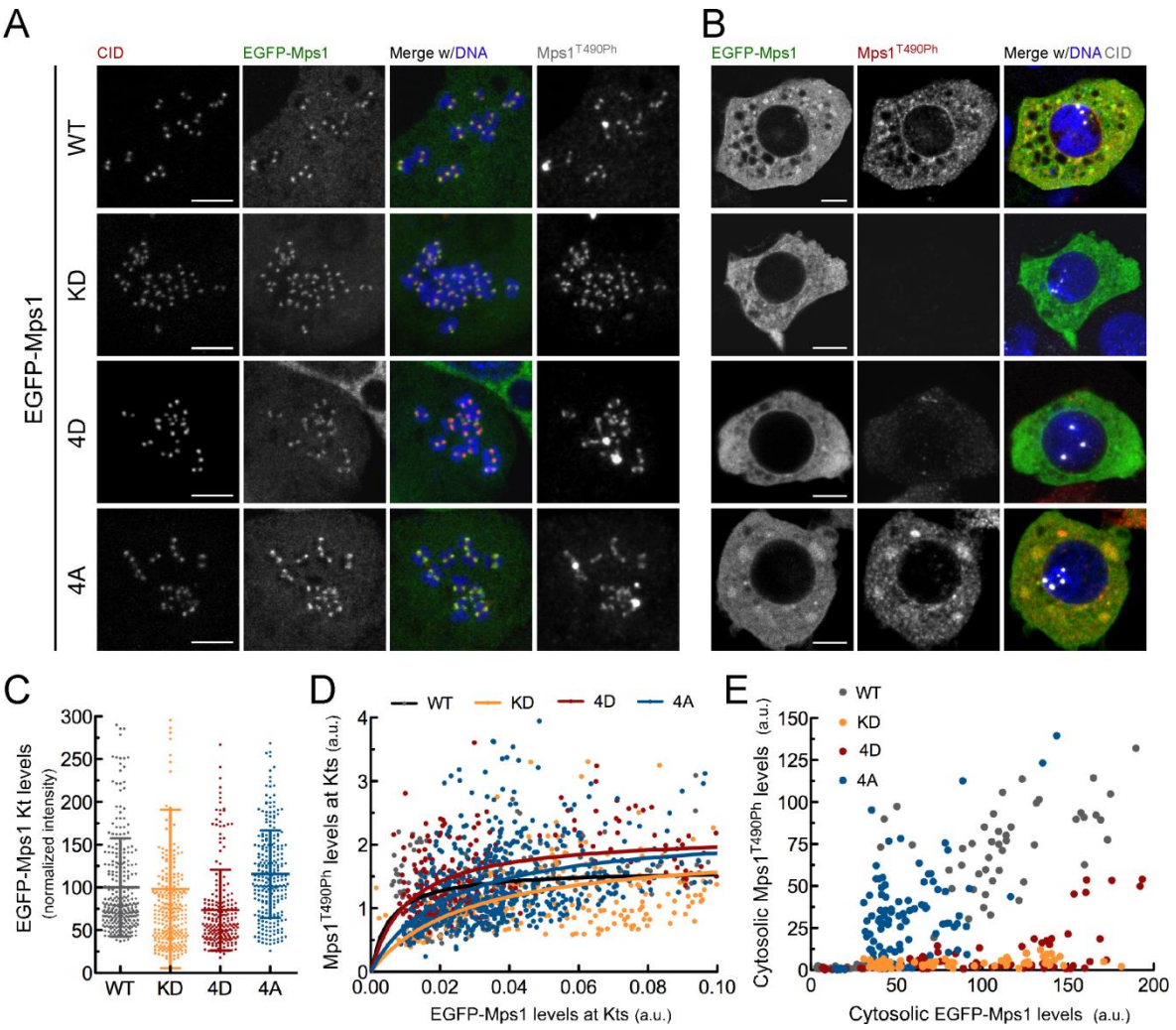

Figure 3.5.1 - Polo phosphorylation of Mps1 N-terminal negatively regulates Mps1 activity. Immunolocalization of EGFP-Mps1 and Mps1^{T490Ph} in prometaphase (A) and interphase cells (B) expressing modified versions of EGFP-Mps1. (C) Quantification of EGFP-Mps1 kinetochore levels from experiment in (A). EGFP-Mps1 fluorescence intensities at kinetochores were corrected for the expression level with cytoplasmic signal and determined relative to CID. Data represent means ± s.d. (D) Quantification of EGFP-Mps1^{T490Ph} kinetochore levels plotted against EGFP-Mps1 kinetochore levels from experiment in (A). Mps1^{T490Ph} fluorescence intensities were determined relative to CID. (E) Quantification of cytosolic EGFP-Mps1^{T490Ph} levels plotted against cytosolic EGFP-Mps1 levels from experiment in (B). For (A), cultured cells were treated with MG132 for 1 hour followed by a 2 hours period of colchicine incubation. Scale bars represent 5 µm.

Overexpression of EGFP-Mps1^{WT} in S2 cells was previously shown to cause a prolonged mitotic delay during metaphase due to persistent SAC activity (Conde et al., 2013a). Live-cell imaging showed that overexpression of EGFP-Mps1^{KD} in S2 cells failed to cause an obvious increase of the mitotic timing, indicating that the observed mitotic arrest resulting from high levels of EGFP-Mps1^{WT} (~ 6.6 hours) depends on Mps1 kinase activity (Figure 3.5.2A). Interestingly, comparing to EGFP-Mps1^{WT}, cells expressing EGFP-

Mps1^{4D} had a less pronounced mitotic delay (~ 3.7 hours) whereas expression of EGFP-Mps1^{4A} resulted in a significant increase of the mitotic timing (~ 8.6 hours) (Figure 3.5.2A). These results parallel the observed effect of the mutations on Mps1 activation assessed by its T-loop phosphorylation in interphase and confirm that Polo-mediated phosphorylation of Mps1 N-terminal region has a negative impact on its catalytic activity. In line with this, expression of an Mps1 version lacking the N-terminal region harboring Polo phosphorylation sites (EGFP-Mps1$^{\Delta 150\text{-}300}$) extended the time spent in mitosis to ~ 10 hours on average (Figure 3.5.2A). Removal of this region likely prevents a regulatory restrain on Mps1 activity, hence maximizing its activation and consequently, prolonging the mitotic arrest. Conversely, co-expression of Polo^{T182D}-EGFP with EGFP-Mps1^{WT} allowed the cells to exit mitosis with an average mitotic timing (~ 4.3 hours) similar to the determined for cells expressing EGFP-Mps1^{4D} (Figure 3.5.2A).

To examine whether Polo-mediated phosphorylation of Mps1 N-terminal restrains Mps1 activation by impairing its dimerization capacity, we immunoprecipitated mutant versions of EGFP-Mps1 and determined the capacity of endogenous Mps1 to co-immunoprecipitate. Immunoblot analysis detected high levels of endogenous Mps1 in EGFP-Mps1^{4D} immunoprecipitates, hence indicating that the mechanism by which Polo negatively regulates Mps1 activity is likely other then precluding Mps1-Mps1 interaction (Figure 3.5.2B).

Because Polo inhibition led to a dramatic increase of Mps1 retention time at kinetochores (Figure 3.3.1F), we examined the impact of N-terminal Polo phosphorylation on Mps1 kinetochore dynamics. FRAP analysis of EGFP-Mps1^{4D} revealed a 2-fold decrease in the half-life of recovery relative to EGFP-Mps1^{WT}, strongly suggesting that Polo phosphorylation of Mps1 N-terminal region promotes Mps1 dissociation from kinetochores (Figure 3.5.2C). Interestingly, co-expression of Polo^{T182D}-EGFP caused a 4-fold decrease of EGFP-Mps1^{WT} half-life of recovery (Figure 3.5.2C). This indicates that additional Polo-controlled mechanisms regulate Mps1 exchange rate at kinetochores. Intriguingly, preventing Polo phosphorylation of EGFP-Mps1 (EGFP-Mps1^{4A}) failed to result in an increase of Mps1 residence time at kinetochores (Figure 3.5.2C). This is likely explained by the dynamics of endogenous Mps1, which is able dimerize with EGFP-Mps1^{4A} (Figure 3.5.2C) and hence contribute for the observed rate at which EGFP-Mps1^{4A} exchanges at kinetochores.

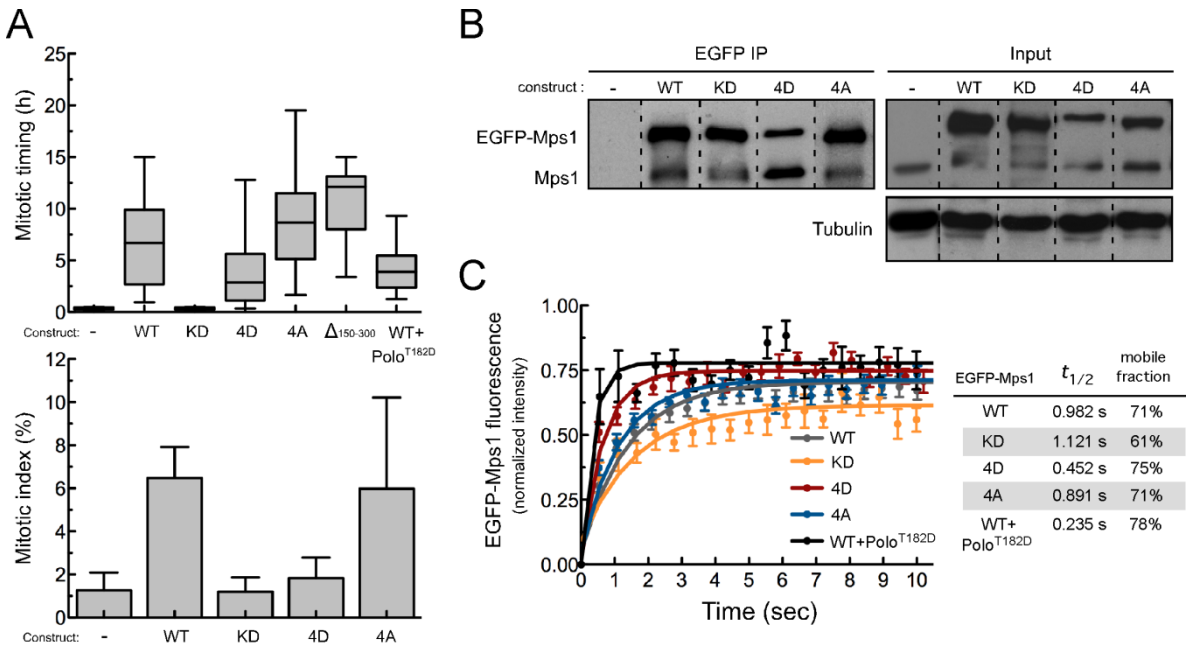

Figure 3.5.2 - Polo phosphorylation of Mps1 N-terminal restrains Mps1 activity and promotes its dissociation from kinetochores. (A) Quantification of the mitotic timing - from nuclear envelope breakdown to mitotic exit - for cells expressing the indicated versions of EGFP-Mps1. In the lower panel, mitotic indexes of cultured cells expressing the indicated EGFP-Mps1 transgenes are depicted. Mitotic indexes were measured in asynchronous cultures 12 hours after $CuSO_4$ addition to induce expression of the transgenes. Mitotic cells were identified by $H3^{Ser10Ph}$ positive staining. (B) Immunoprecipitation of EGFP-Mps1 from total cell lysates obtained from S2 cells expressing EGFP-$Mps1^{WT}$, EGFP-$Mps1^{KD}$, EGFP-$Mps1^{4D}$ and EGFP-$Mps1^{4A}$. Immunoprecipitates (IP) and corresponding total cell lysates (Input) were probed by immunoblotting for the indicated proteins. (C) FRAP analysis of different versions of EGFP-Mps1 after bleaching of single kinetochores. Graph shows average fluorescence intensities ± s.e. n= 20 cells/condition. Recovery half-life and mobile fraction are depicted. For (B) and (C) cultured cells were treated with MG132 for 1 hour followed by a 2 hours period of colchicine incubation.

Taken together, the results obtained in this work indicate that Polo exerts a dual regulation over Mps1 activity, hence defining SAC robustness and responsiveness. Polo promotes Mps1 activation at the nuclear envelope/pore and its subsequent nuclear import during prophase, which likely leads to auto-phosphorylation dependent Mps1 recruitment to prometaphase kinetochores required for robust SAC function. During prometaphase, Polo activity is continuously required to maintain Mps1 active at kinetochores. Mps1 in its active conformation exposes its N-terminal domain that becomes phosphorylated by Polo. Polo-mediated phosphorylation of Mps1 N-terminal region restrains Mps1 activity and promotes its prompt dissociation from kinetochores. This allows fast SAC silencing upon biorientation, hereby providing SAC responsiveness.

CHAPTER 4

GENERAL DISCUSSION

Proper SAC signalling is crucial to genomic stability because it prevents chromosome segregation and progression through mitosis until all chromosomes are properly attached to the mitotic spindle. A remarkable feature of the SAC is that a single unattached kinetochore is able to generate a signal strong enough to delay anaphase. Yet cells rapidly silence SAC activity and separate their sister chromatids once all chromosomes attain biorientation. How the SAC can be simultaneously highly responsive and robust remains poorly understood. An intricate kinase network present at kinetochores connected by multiple positive feedback loops creates a robust SAC response that is promptly silenced upon microtubule attachments by the action of antagonizing phosphatases. This is thought to allow the tight coupling between kinetochore-microtubule attachment status and SAC signalling, thus ensuring prompt metaphase-anaphase transition upon biorientation of all chromosomes. Interestingly, the results presented in this thesis strongly support that Polo exerts a dual regulation over Mps1 activity that further contributes to define SAC robustness and responsiveness.

Polo and its orthologues are key mitotic regulators. Early work showing that Polo kinases become enriched at kinetochores in prometaphase cells (Arnaud et al., 1998; Golsteyn et al., 1995) led to the hypothesis that it could play an important role in SAC function. However, subsequent studies failed to demonstrate a clear role for Polo kinases in SAC signalling. Plx1 was shown to be required for SAC function in *Xenopus* as the kinase responsible for 3F3/2 formation at tensionless kinetochores (Wong & Fang, 2007). However, in human cells, Plk1 seems to be dispensable for SAC activity as its inhibition or depletion resulted in a SAC-dependent prometaphase arrest with accumulation of Mad2 and BubR1 at kinetochores (Sumara *et al*, 2004; Lénárt *et al*, 2007; Petronczki *et al*, 2008). This contrasts with other studies that reported a substantial reduction of kinetochore-associated levels of Mad1, Mad2 and Cdc20, upon down-regulation of Plk1, suggesting a role for Plk1 in SAC regulation (Ahonen *et al*, 2005; Chi *et al*, 2008). Important insights into this controversy were recently provided by results obtained in *Drosophila*. In S2 cells, Polo was shown to be required for proper Mps1-dependent SAC signalling (Conde et al., 2013a). The accumulation of Mps1 at unattached kinetochores is essential for its full activation and consequently to ensure sustained SAC function (Heinrich et al., 2012; Santaguida et al., 2011; Saurin et al., 2011). Conde and colleagues have shown that Mps1 localization at unattached kinetochores is negatively affected in Polo-depleted cells (Conde et al., 2013a). Polo appears to promote proper Mps1

recruitment indirectly by controlling Aurora B activity and Ndc80 kinetochore localization (Conde et al., 2013a).

In this work, by using a phosphospecific antibody that recognizes the activating Mps1-T-loop autophosphorylation ($Mps1^{T490Ph}$) we confirmed that Polo depletion from S2 cells impairs proper Mps1 activation at kinetochores. A similar decrease in Mps1 activity was observed when Polo kinase was inhibited with BI2536. However, and markedly contrasting with RNAi-mediated Polo depletion, in this situation, Mps1 levels at kinetochores were severely incremented. Our results strongly suggest that this is the outcome of a dramatic decrease in Mps1 dynamic exchange at kinetochores as assessed by FRAP. Importantly, these results in the retention of high levels of inactive Mps1 at kinetochores that are stably attached to spindle microtubules in a syntelic fashion further supporting the notion that Polo activity is required for Mps1 release from kinetochores. The regulation of Mps1 dynamics at kinetochores by Polo is likely direct, since impairing Mps1 activation or preventing PP2A-B56α kinetochore localization without affecting Polo activity only marginally affected Mps1 dynamics.

These results provide another important insight towards the understanding of Mps1 activation. The observation that in the absence of Polo activity, Mps1 is retained at high levels at kinetochores in an inactive state and that its dimerization capacity remains unaffected, reveals that kinetochore accumulation of endogenous Mps1 and its dimerization are not sufficient to drive its activation in prometaphase cells and that other factors such as Polo activity, are required for the process.

The obvious discrepancy between Polo depletion and inhibition on Mps1 kinetochore recruitment might relate to Polo as a structural receptor of Mps1 rather than a requirement of its catalytic activity. However, two lines of evidence argue against this. Kinetochore levels of Polo failed to increase to the extent observed for Mps1 upon BI2536 treatment (Luis Santos, unpublished data). Moreover, and consistent with a direct role of Ndc80 as a kinetochore receptor for Mps1 (Conde et al., 2013a), its depletion results in more dramatic effects on Mps1 recruitment (to 10%) than Polo depletion (to 40%). It should be noted that Polo inhibition caused a slight reduction of Ndc80 levels at kinetochores, hence indicating that the observed increase in Mps1 kinetochore association is not driven by an increase of its previously established receptor (Conde et al., 2013a).

The observation that a kinase-dead version of Mps1 is unable to localize at unattached kinetochores in the absence of endogenous Mps1 indicates that Mps1 activity is required for its kinetochore recruitment in *Drosophila* (Althoff et al., 2012). Intriguingly,

loss of Mps1 activity due to Polo inhibition caused an overaccumulation of Mps1 at kinetochores. We speculate that the timing at which cells loose Polo activity likely explains the observed discrepancy between RNAi-mediated depletion of Polo and inhibition of its activity with BI2536. Analyzed mitotic cells depleted of Polo had likely entered mitosis already in the absence of Polo activity, whereas the mitotic cells from cultures treated with BI2536 have probably lost Polo activity when already in mitosis. We found that in S2 cells, Polo inhibition with BI2536 at the G2/M transition strongly impairs mitotic entry during the time-frame of our assay (Carlos Conde, unpublished). In this way, the vast majority of BI2536 mitotic cells analyzed were mandatorily in mitosis when the drug was added to cultures. This indicates that loss of Polo activity before mitotic entry impairs Mps1 recruitment to kinetochores, whereas its inhibition upon mitotic entry prevents its release from these sites.

Mps1 accumulation at kinetochores is thought to facilitate its dimerization and consequently promote its full activation through trans-autophosphorylation of the kinase T-loop (Conde et al., 2013b). However, the fact that Mps1 activity is required for its own kinetochore localization in flies, implicates that Mps1 activity also needs to increase prior to its localization to kinetochores. Our results strongly suggest that during prophase, Polo activity contributes to the initial activation of Mps1 required to drive the bulk of its kinetochore recruitment upon NEB. Moreover, our data indicates that this process may take place at the nuclear envelope/pore and that Polo promotes the nuclear import of active Mps1 immediately before mitotic entry. Firstly, Mps1 and active Polo are present at the nuclear envelope/pore at this stage. Secondly, depletion of Polo led to a reduction in the levels of active Mps1 in the nucleoplasm of prophase cells. Thirdly, expression of constitutively active Polo during interphase was able to drive activation of endogenous Mps1 and promote its nuclear import. Lastly, Mps1 overexpression in interphase also resulted in Mps1 activation but fails to promote its import to the nucleus, suggesting a Polo-specific role in this process rather than a consequence of Mps1 activation. The relevance of Mps1 nuclear import in its active form for its kinetochore recruitment is currently being addressed in the lab.

Interestingly Polo and Mps1 interact *in vivo* and *in vitro* kinase assays showed that Polo is able to phosphorylate Mps1 in its N-terminal region. Mps1 N-terminal region constitutes a disordered domain inaccessible to Polo when Mps1 is in its inactive state. However, Mps1 autophosphorylation likely induces a structural rearrangement exposing the previously cryptic N-terminal region, which, consequently becomes phosphorylated by

Polo. We are currently identifying Polo phosphorylation sites on Mps1 by means of LC-ESI-MS/MS. Nevertheless, *in silico* analysis predicts the existence of 4 putative Polo phosphorylation sites (Thr^{185}, Thr^{197}, Thr^{260}, Ser^{262}) within the Mps1 N-terminal, whose relevance for Mps1 activity we decided to evaluate.

We found that mimicking Polo phosphorylation of Mps1 N-terminal region decreased Mps1 residence time at kinetochores and caused a small but significant reduction of its recruitment to unattached kinetochores. Interestingly, mimicking Polo phosphorylation did not prevent Mps1 dimerization, but nevertheless had a negative impact on the capacity to induce kinase activation when overexpressed during interphase. Accordingly, EGFP-$Mps1^{4D}$ failed to cause a mitotic arrest to the same extent of its wild-type counterpart. On the other hand, expression of a phosphodefective version of Mps1 for the putative Polo phosphorylation sites facilitated Mps1 activation in interphase and extended the time these cells arrest in mitosis. In accordance, removal of this region led to a significant increase of Mps1 activity. Cumulatively, these findings strongly suggest that Polo-mediated phosphorylation of Mps1 N-terminal region induces a regulatory restrain on Mps1 activity, negatively affecting its activation at kinetochores and promoting its dissociation from these structures.

Structural studies will be critical to understand how the N-terminal region of Mps1 restrains its catalytic activity. The most straightforward mechanism that we envision is one in which the N-terminal interacts with the kinase domain, inhibiting its accessibility to substrates or preventing its T-loop phosphorylation. Our results suggest that Polo can only phosphorylate Mps1 N-terminal when Mps1 is in its active state indicating that instead of preventing Mps1 activation, Polo acts to restrain it at kinetochores. Paradoxically, Polo activity is also required to promote initial Mps1 activation and sustain its active state during prometaphase. However, the inability of Polo to phosphorylate catalytic inactive Mps1 suggests that the mechanism by which Polo contributes for its initial activation during prophase is either indirect or requires additional factors. Likewise, the requirement of Polo activity for continuous Mps1 activation at kinetochore underlies the role of Polo in controlling proper Aurora B centromeric localization and activity. Therefore, Polo indirectly promotes Mps1 activation and kinetochore localization and directly restrains its activity and directs its dissociation from kinetochores (Figure 4.1). What is the relevance of such a dual regulation of Mps1 activity exerted by Polo?

By triggering Mps1 activation at the nuclear envelope/pore in prophase, Polo indirectly promotes the initial recruitment of Mps1 to unattached kinetochores in early

mitosis. This likely increments further Mps1 localization and activation at kinetochores due to the dimerization capacity of Mps1 and allows the cell to promptly establish robust SAC signalling and efficient production of MCC. At unattached kinetochores, Polo activity is continuously required to maintain Mps1 activation by controlling Aurora B localization and activity. On the other hand, Polo is able to phosphorylate active Mps1 in its N-terminal region to restrain its activity and promote its dissociation from kinetochores. Because the inhibitory Polo phosphorylations can only occur once Mps1 assumes its active conformation an equilibrium state is established that sets the SAC signal strong as long as Aurora B activity remains elevated. In this way, Polo contributes to prevent Mps1 hyperactivation and for its removal from kinetochores. This allows fast SAC silencing upon biorientation, hereby providing SAC responsiveness.

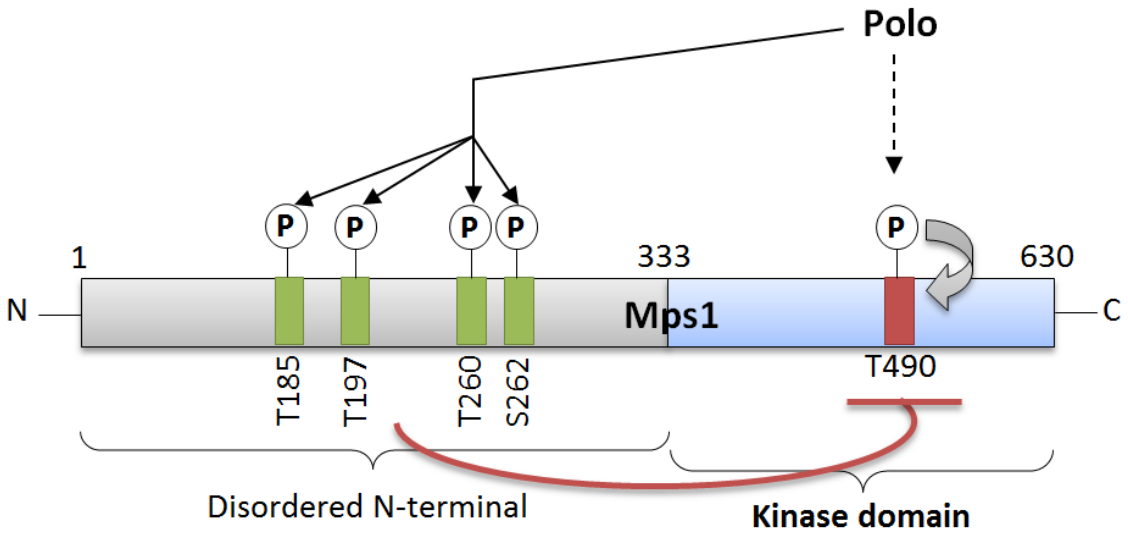

Figure 4.1 - Polo exerts a dual regulation over Mps1 activity to define SAC robustness and responsiveness. Polo promotes Mps1 activation at the nuclear envelope/pore and its subsequent nuclear import during prophase, which likely leads to auto-phosphorylation dependent Mps1 recruitment to prometaphase kinetochores required for robust SAC function. During prometaphase, Polo activity is continuously required to maintain Mps1 active at kinetochores. Mps1 in its active conformation exposes its N-terminal domain that becomes phosphorylated by Polo. Polo-mediated phosphorylation of Mps1 N-terminal region restrains Mps1 activity and promotes its prompt dissociation from kinetochores. This allows fast SAC silencing upon biorientation, hereby providing SAC responsiveness.

CHAPTER 5

REFERENCES

Ahonen, L.J., M.J. Kallio, J.R. Daum, M. Bolton, I.A. Manke, M.B. Yaffe, P.T. Stukenberg, and G.J. Gorbsky. 2005. Polo-like kinase 1 creates the tension-sensing 3F3/2 phosphoepitope and modulates the association of spindle-checkpoint proteins at kinetochores. *Current biology : CB*. 15:1078-1089.

Althoff, F., R.E. Karess, and C.F. Lehner. 2012. Spindle checkpoint-independent inhibition of mitotic chromosome segregation by Drosophila Mps1. *Molecular biology of the cell*. 23:2275-2291.

Archambault, V., and D.M. Glover. 2009. Polo-like kinases: conservation and divergence in their functions and regulation. *Nature reviews. Molecular cell biology*. 10:265-275.

Arnaud, L., J. Pines, and E.A. Nigg. 1998. GFP tagging reveals human Polo-like kinase 1 at the kinetochore/centromere region of mitotic chromosomes. *Chromosoma*. 107:424-429.

Bayliss, R., A. Fry, T. Haq, and S. Yeoh. 2012. On the molecular mechanisms of mitotic kinase activation. *Open biology*. 2:120136.

Bruinsma, W., J.A. Raaijmakers, and R.H. Medema. 2012. Switching Polo-like kinase-1 on and off in time and space. *Trends in biochemical sciences*. 37:534-542.

Carmena, M., X. Pinson, M. Platani, Z. Salloum, Z. Xu, A. Clark, F. Macisaac, H. Ogawa, U. Eggert, D.M. Glover, V. Archambault, and W.C. Earnshaw. 2012. The chromosomal passenger complex activates Polo kinase at centromeres. *PLoS biology*. 10:e1001250.

Cheeseman, I.M., and A. Desai. 2008. Molecular architecture of the kinetochore-microtubule interface. *Nature reviews. Molecular cell biology*. 9:33-46.

Chi, Y.H., K. Haller, M.D. Ward, O.J. Semmes, Y. Li, and K.T. Jeang. 2008. Requirements for protein phosphorylation and the kinase activity of polo-like kinase 1 (Plk1) for the kinetochore function of mitotic arrest deficiency protein 1 (Mad1). *The Journal of biological chemistry*. 283:35834-35844.

Colombo, R., M. Caldarelli, M. Mennecozzi, M.L. Giorgini, F. Sola, P. Cappella, C. Perrera, S.R. Depaolini, L. Rusconi, U. Cucchi, N. Avanzi, J.A. Bertrand, R.T. Bossi, E. Pesenti, A. Galvani, A. Isacchi, F. Colotta, D. Donati, and J. Moll. 2010. Targeting the mitotic checkpoint for cancer therapy with NMS-P715, an inhibitor of MPS1 kinase. *Cancer research*. 70:10255-10264.

Conde, C., M. Osswald, J. Barbosa, T. Moutinho-Santos, D. Pinheiro, S. Guimaraes, I. Matos, H. Maiato, and C.E. Sunkel. 2013a. Drosophila Polo regulates the spindle assembly checkpoint through Mps1-dependent BubR1 phosphorylation. *The EMBO journal*. 32:1761-1777.

Conde, C., M. Osswald, and C.E. Sunkel. 2013b. All together now: Polo joins the kinase network controlling the spindle assembly checkpoint in Drosophila. *Fly*. 7:224-228.

Davenport, J., L.D. Harris, and R. Goorha. 2006. Spindle checkpoint function requires Mad2-dependent Cdc20 binding to the Mad3 homology domain of BubR1. *Experimental cell research*. 312:1831-1842.

De Antoni, A., C.G. Pearson, D. Cimini, J.C. Canman, V. Sala, L. Nezi, M. Mapelli, L. Sironi, M. Faretta, E.D. Salmon, and A. Musacchio. 2005. The Mad1/Mad2 complex as a template for Mad2 activation in the spindle assembly checkpoint. *Current biology : CB*. 15:214-225.

Elowe, S., S. Hummer, A. Uldschmid, X. Li, and E.A. Nigg. 2007. Tension-sensitive Plk1 phosphorylation on BubR1 regulates the stability of kinetochore microtubule interactions. *Genes & development*. 21:2205-2219.

Fitzgerald, D.J., P. Berger, C. Schaffitzel, K. Yamada, T.J. Richmond, and I. Berger. 2006. Protein complex expression by using multigene baculoviral vectors. *Nature methods*. 3:1021-1032.

Gavet, O., and J. Pines. 2010. Progressive activation of CyclinB1-Cdk1 coordinates entry to mitosis. *Developmental cell*. 18:533-543.

Golsteyn, R.M., K.E. Mundt, A.M. Fry, and E.A. Nigg. 1995. Cell cycle regulation of the activity and subcellular localization of Plk1, a human protein kinase implicated in mitotic spindle function. *The Journal of cell biology*. 129:1617-1628.

Hagting, A., N. Den Elzen, H.C. Vodermaier, I.C. Waizenegger, J.M. Peters, and J. Pines. 2002. Human securin proteolysis is controlled by the spindle checkpoint and reveals when the APC/C switches from activation by Cdc20 to Cdh1. *The Journal of cell biology*. 157:1125-1137.

Hardwick, K.G., and A.W. Murray. 1995. Mad1p, a phosphoprotein component of the spindle assembly checkpoint in budding yeast. *The Journal of cell biology*. 131:709-720.

Hartwell, L.H., R.K. Mortimer, J. Culotti, and M. Culotti. 1973. Genetic Control of the Cell Division Cycle in Yeast: V. Genetic Analysis of cdc Mutants. *Genetics*. 74:267-286.

Heinrich, S., H. Windecker, N. Hustedt, and S. Hauf. 2012. Mph1 kinetochore localization is crucial and upstream in the hierarchy of spindle assembly checkpoint protein recruitment to kinetochores. *Journal of cell science*. 125:4720-4727.

Hewitt, L., A. Tighe, S. Santaguida, A.M. White, C.D. Jones, A. Musacchio, S. Green, and S.S. Taylor. 2010. Sustained Mps1 activity is required in mitosis to recruit O-Mad2 to the Mad1-C-Mad2 core complex. *The Journal of cell biology*. 190:25-34.

Holland, A.J., and D.W. Cleveland. 2012. Losing balance: the origin and impact of aneuploidy in cancer. *EMBO reports*. 13:501-514.

Huang, H., J. Hittle, F. Zappacosta, R.S. Annan, A. Hershko, and T.J. Yen. 2008. Phosphorylation sites in BubR1 that regulate kinetochore attachment, tension, and mitotic exit. *The Journal of cell biology*. 183:667-680.

Jang, Y.J., C.Y. Lin, S. Ma, and R.L. Erikson. 2002. Functional studies on the role of the C-terminal domain of mammalian polo-like kinase. *Proceedings of the National Academy of Sciences of the United States of America*. 99:1984-1989.

Jelluma, N., A.B. Brenkman, I. McLeod, J.R. Yates, 3rd, D.W. Cleveland, R.H. Medema, and G.J. Kops. 2008. Chromosomal instability by inefficient Mps1 auto-activation due to a weakened mitotic checkpoint and lagging chromosomes. *PloS one*. 3:e2415.

Jelluma, N., T.B. Dansen, T. Sliedrecht, N.P. Kwiatkowski, and G.J. Kops. 2010. Release of Mps1 from kinetochores is crucial for timely anaphase onset. *The Journal of cell biology*. 191:281-290.

Kang, J., Y. Chen, Y. Zhao, and H. Yu. 2007. Autophosphorylation-dependent activation of human Mps1 is required for the spindle checkpoint. *Proceedings of the National Academy of Sciences of the United States of America*. 104:20232-20237.

King, R.W., J.M. Peters, S. Tugendreich, M. Rolfe, P. Hieter, and M.W. Kirschner. 1995. A 20S complex containing CDC27 and CDC16 catalyzes the mitosis-specific conjugation of ubiquitin to cyclin B. *Cell*. 81:279-288.

Kulukian, A., J.S. Han, and D.W. Cleveland. 2009. Unattached kinetochores catalyze production of an anaphase inhibitor that requires a Mad2 template to prime Cdc20 for BubR1 binding. *Developmental cell*. 16:105-117.

Kwiatkowski, N., N. Jelluma, P. Filippakopoulos, M. Soundararajan, M.S. Manak, M. Kwon, H.G. Choi, T. Sim, Q.L. Deveraux, S. Rottmann, D. Pellman, J.V. Shah, G.J. Kops, S. Knapp, and N.S. Gray. 2010. Small-molecule kinase inhibitors provide insight into Mps1 cell cycle function. *Nature chemical biology*. 6:359-368.

Lan, W., and D.W. Cleveland. 2010. A chemical tool box defines mitotic and interphase roles for Mps1 kinase. *The Journal of cell biology*. 190:21-24.

Lara-Gonzalez, P., F.G. Westhorpe, and S.S. Taylor. 2012. The spindle assembly checkpoint. *Current biology : CB*. 22:R966-980.

Lenart, P., M. Petronczki, M. Steegmaier, B. Di Fiore, J.J. Lipp, M. Hoffmann, W.J. Rettig, N. Kraut, and J.M. Peters. 2007. The small-molecule inhibitor BI 2536 reveals novel insights into mitotic roles of polo-like kinase 1. *Current biology : CB*. 17:304-315.

Liu, S.T., G.K. Chan, J.C. Hittle, G. Fujii, E. Lees, and T.J. Yen. 2003. Human MPS1 kinase is required for mitotic arrest induced by the loss of CENP-E from kinetochores. *Molecular biology of the cell*. 14:1638-1651.

Liu, X., and M. Winey. 2012. The MPS1 family of protein kinases. *Annual review of biochemistry*. 81:561-585.

London, N., S. Ceto, J.A. Ranish, and S. Biggins. 2012. Phosphoregulation of Spc105 by Mps1 and PP1 regulates Bub1 localization to kinetochores. *Current biology : CB*. 22:900-906.

Lowery, D.M., D. Lim, and M.B. Yaffe. 2005. Structure and function of Polo-like kinases. *Oncogene*. 24:248-259.

Maciejowski, J., K.A. George, M.E. Terret, C. Zhang, K.M. Shokat, and P.V. Jallepalli. 2010. Mps1 directs the assembly of Cdc20 inhibitory complexes during interphase and mitosis to control M phase timing and spindle checkpoint signaling. *The Journal of cell biology*. 190:89-100.

Macurek, L., A. Lindqvist, D. Lim, M.A. Lampson, R. Klompmaker, R. Freire, C. Clouin, S.S. Taylor, M.B. Yaffe, and R.H. Medema. 2008. Polo-like kinase-1 is activated by aurora A to promote checkpoint recovery. *Nature*. 455:119-123.

Maia, A.F., C.S. Lopes, and C.E. Sunkel. 2007. BubR1 and CENP-E have antagonistic effects upon the stability of microtubule-kinetochore attachments in Drosophila S2 cell mitosis. *Cell cycle*. 6:1367-1378.

Malureanu, L.A., K.B. Jeganathan, M. Hamada, L. Wasilewski, J. Davenport, and J.M. van Deursen. 2009. BubR1 N terminus acts as a soluble inhibitor of cyclin B degradation by APC/C(Cdc20) in interphase. *Developmental cell*. 16:118-131.

Mapelli, M., L. Massimiliano, S. Santaguida, and A. Musacchio. 2007. The Mad2 conformational dimer: structure and implications for the spindle assembly checkpoint. *Cell*. 131:730-743.

Martins, T., A.F. Maia, S. Steffensen, and C.E. Sunkel. 2009. Sgt1, a co-chaperone of Hsp90 stabilizes Polo and is required for centrosome organization. *The EMBO journal*. 28:234-247.

Matsumura, S., F. Toyoshima, and E. Nishida. 2007. Polo-like kinase 1 facilitates chromosome alignment during prometaphase through BubR1. *The Journal of biological chemistry*. 282:15217-15227.

Mattison, C.P., W.M. Old, E. Steiner, B.J. Huneycutt, K.A. Resing, N.G. Ahn, and M. Winey. 2007. Mps1 activation loop autophosphorylation enhances kinase activity. *The Journal of biological chemistry*. 282:30553-30561.

McKinley, K.L., and I.M. Cheeseman. 2014. Polo-like kinase 1 licenses CENP-A deposition at centromeres. *Cell*. 158:397-411.

Mitchison, T.J., and E.D. Salmon. 2001. Mitosis: a history of division. *Nature cell biology*. 3:E17-21.

Morgan, D. 2007. The Cell Cycle. Oxford University Press.

Moutinho-Santos, T., C. Conde, and C.E. Sunkel. 2012. POLO ensures chromosome bi-orientation by preventing and correcting erroneous chromosome-spindle attachments. *Journal of cell science*. 125:576-583.

Nijenhuis, W., E. von Castelmur, D. Littler, V. De Marco, E. Tromer, M. Vleugel, M.H. van Osch, B. Snel, A. Perrakis, and G.J. Kops. 2013. A TPR domain-containing N-

terminal module of MPS1 is required for its kinetochore localization by Aurora B. *The Journal of cell biology*. 201:217-231.

Page, S.L., R.J. Nielsen, K. Teeter, C.M. Lake, S. Ong, K.R. Wright, K.L. Dean, D. Agne, W.D. Gilliland, and R.S. Hawley. 2007. A germline clone screen for meiotic mutants in Drosophila melanogaster. *Fly*. 1:172-181.

Petronczki, M., P. Lenart, and J.M. Peters. 2008. Polo on the Rise-from Mitotic Entry to Cytokinesis with Plk1. *Developmental cell*. 14:646-659.

Pike, A.N., and H.A. Fisk. 2011. Centriole assembly and the role of Mps1: defensible or dispensable? *Cell division*. 6:9.

Pines, J. 2011. Cubism and the cell cycle: the many faces of the APC/C. *Nature reviews. Molecular cell biology*. 12:427-438.

Primorac, I., J.R. Weir, E. Chiroli, F. Gross, I. Hoffmann, S. van Gerwen, A. Ciliberto, and A. Musacchio. 2013. Bub3 reads phosphorylated MELT repeats to promote spindle assembly checkpoint signaling. *eLife*. 2:e01030.

Rieder, C.L., R.W. Cole, A. Khodjakov, and G. Sluder. 1995. The checkpoint delaying anaphase in response to chromosome monoorientation is mediated by an inhibitory signal produced by unattached kinetochores. *The Journal of cell biology*. 130:941-948.

Rieder, C.L., A. Schultz, R. Cole, and G. Sluder. 1994. Anaphase onset in vertebrate somatic cells is controlled by a checkpoint that monitors sister kinetochore attachment to the spindle. *The Journal of cell biology*. 127:1301-1310.

Santaguida, S., A. Tighe, A.M. D'Alise, S.S. Taylor, and A. Musacchio. 2010. Dissecting the role of MPS1 in chromosome biorientation and the spindle checkpoint through the small molecule inhibitor reversine. *The Journal of cell biology*. 190:73-87.

Santaguida, S., C. Vernieri, F. Villa, A. Ciliberto, and A. Musacchio. 2011. Evidence that Aurora B is implicated in spindle checkpoint signalling independently of error correction. *The EMBO journal*. 30:1508-1519.

Saurin, A.T., M.S. van der Waal, R.H. Medema, S.M. Lens, and G.J. Kops. 2011. Aurora B potentiates Mps1 activation to ensure rapid checkpoint establishment at the onset of mitosis. *Nature communications*. 2:316.

Sczaniecka, M., A. Feoktistova, K.M. May, J.S. Chen, J. Blyth, K.L. Gould, and K.G. Hardwick. 2008. The spindle checkpoint functions of Mad3 and Mad2 depend on a Mad3 KEN box-mediated interaction with Cdc20-anaphase-promoting complex (APC/C). *The Journal of biological chemistry*. 283:23039-23047.

Seki, A., J.A. Coppinger, C.Y. Jang, J.R. Yates, and G. Fang. 2008. Bora and the kinase Aurora a cooperatively activate the kinase Plk1 and control mitotic entry. *Science*. 320:1655-1658.

Shepperd, L.A., J.C. Meadows, A.M. Sochaj, T.C. Lancaster, J. Zou, G.J. Buttrick, J. Rappsilber, K.G. Hardwick, and J.B. Millar. 2012. Phosphodependent recruitment of Bub1 and Bub3 to Spc7/KNL1 by Mph1 kinase maintains the spindle checkpoint. *Current biology : CB*. 22:891-899.

Simonetta, M., R. Manzoni, R. Mosca, M. Mapelli, L. Massimiliano, M. Vink, B. Novak, A. Musacchio, and A. Ciliberto. 2009. The influence of catalysis on mad2 activation dynamics. *PLoS biology*. 7:e10.

Stucke, V.M., C. Baumann, and E.A. Nigg. 2004. Kinetochore localization and microtubule interaction of the human spindle checkpoint kinase Mps1. *Chromosoma*. 113:1-15.

Stucke, V.M., H.H. Sillje, L. Arnaud, and E.A. Nigg. 2002. Human Mps1 kinase is required for the spindle assembly checkpoint but not for centrosome duplication. *The EMBO journal*. 21:1723-1732.

Suijkerbuijk, S.J., M. Vleugel, A. Teixeira, and G.J. Kops. 2012. Integration of kinase and phosphatase activities by BUBR1 ensures formation of stable kinetochore-microtubule attachments. *Developmental cell*. 23:745-755.

Sumara, I., J.F. Gimenez-Abian, D. Gerlich, T. Hirota, C. Kraft, C. de la Torre, J. Ellenberg, and J.M. Peters. 2004. Roles of polo-like kinase 1 in the assembly of functional mitotic spindles. *Current biology : CB*. 14:1712-1722.

Sunkel, C.E., and D.M. Glover. 1988. polo, a mitotic mutant of Drosophila displaying abnormal spindle poles. *Journal of cell science*. 89 (Pt 1):25-38.

Trowitzsch, S., C. Bieniossek, Y. Nie, F. Garzoni, and I. Berger. 2010. New baculovirus expression tools for recombinant protein complex production. *Journal of structural biology*. 172:45-54.

van de Weerdt, B.C., M.A. van Vugt, C. Lindon, J.J. Kauw, M.J. Rozendaal, R. Klompmaker, R.M. Wolthuis, and R.H. Medema. 2005. Uncoupling anaphase-promoting complex/cyclosome activity from spindle assembly checkpoint control by deregulating polo-like kinase 1. *Molecular and cellular biology*. 25:2031-2044.

Virshup, D.M., and P. Kaldis. 2010. Cell biology. Enforcing the Greatwall in mitosis. *Science*. 330:1638-1639.

Vleugel, M., E. Hoogendoorn, B. Snel, and G.J. Kops. 2012. Evolution and function of the mitotic checkpoint. *Developmental cell*. 23:239-250.

Wang, W., Y. Yang, Y. Gao, Q. Xu, F. Wang, S. Zhu, W. Old, K. Resing, N. Ahn, M. Lei, and X. Liu. 2009. Structural and mechanistic insights into Mps1 kinase activation. *Journal of cellular and molecular medicine*. 13:1679-1694.

Wolf, F., C. Wandke, N. Isenberg, and S. Geley. 2006. Dose-dependent effects of stable cyclin B1 on progression through mitosis in human cells. *The EMBO journal*. 25:2802-2813.

Wong, O.K., and G. Fang. 2005. Plx1 is the 3F3/2 kinase responsible for targeting spindle checkpoint proteins to kinetochores. *The Journal of cell biology*. 170:709-719.

Xu, Q., S. Zhu, W. Wang, X. Zhang, W. Old, N. Ahn, and X. Liu. 2009. Regulation of kinetochore recruitment of two essential mitotic spindle checkpoint proteins by Mps1 phosphorylation. *Molecular biology of the cell*. 20:10-20.

Yamagishi, Y., C.H. Yang, Y. Tanno, and Y. Watanabe. 2012. MPS1/Mph1 phosphorylates the kinetochore protein KNL1/Spc7 to recruit SAC components. *Nature cell biology*. 14:746-752.

Zhao, Y., and R.H. Chen. 2006. Mps1 phosphorylation by MAP kinase is required for kinetochore localization of spindle-checkpoint proteins. *Current biology : CB*. 16:1764-1769.

Zich, J., A.M. Sochaj, H.M. Syred, L. Milne, A.G. Cook, H. Ohkura, J. Rappsilber, and K.G. Hardwick. 2012. Kinase activity of fission yeast Mph1 is required for Mad2 and Mad3 to stably bind the anaphase promoting complex. *Current biology : CB*. 22:296-301.

Zitouni, S., C. Nabais, S.C. Jana, A. Guerrero, and M. Bettencourt-Dias. 2014. Polo-like kinases: structural variations lead to multiple functions. *Nature reviews. Molecular cell biology*. 15:433-452.